

Supplementary Information

Synthesis and fluorescence properties of 9,9-dimethylfluorene-diyl bridged molecular gyrotops: Effects of slight fluorophore motion on fluorescence efficiency in a solid-state

Reina Yoshizawa,^a Yusuke Inagaki,^a Hiroyuki Momma,^b Eunsang Kwon,^b Kazuaki Ohara,^c Kentaro Yamaguchi,^c and Wataru Setaka*^a

a. Division of Applied Chemistry, Faculty of Urban Environmental Sciences, Tokyo Metropolitan University, Hachioji, Tokyo 192-0397, Japan

b. Faculty of Pharmaceutic Research and Analytical Center for Giant Molecules, Graduate School of Science, Tohoku University, Aoba-ku, Sendai, 980-8578, Japan.

c. Faculty of Pharmaceutical Sciences at Kagawa Campus, Tokushima Bunri University, 1314-1 Shido, Sanuki, Kagawa 769-2193, Japan.

E-mail: wsetaka@tmu.ac.jp

(Total 26 pages including this cover page)

1. Copies of NMR and HRMS Spectra for New Compounds

- Fig. S1.** ¹H NMR spectrum of **C10FluC10** in CDCl₃.
Fig. S2. ¹³C NMR spectrum of **C10FluC10** in CDCl₃.
Fig. S3. HRMS spectrum of **C10FluC10** (ESI, positive). Top: obsd. Bottom: sim.
Fig. S4. ¹H NMR spectrum of **C12FluC12** in CDCl₃.
Fig. S5. ¹³C NMR spectrum of **C12FluC12** in CDCl₃.
Fig. S6. HRMS spectrum of **C12FluC12** (ESI, positive). Top: obsd. Bottom: sim.
Fig. S7. ¹H NMR spectrum of **C18** in CDCl₃.
Fig. S8. ¹³C NMR spectrum of **C18** in CDCl₃.
Fig. S9. HRMS spectrum of **C18** (ESI, positive). Top: obsd. Bottom: sim.
Fig. S10. ¹H NMR spectrum of **C18i** in CDCl₃.
Fig. S11. ¹³C NMR spectrum of **C18i** in CDCl₃.
Fig. S12. HRMS spectrum of **C18i** (ESI, positive). Top: obsd. Bottom: sim.
Fig. S13. ¹H NMR spectrum of **C22** in CDCl₃.
Fig. S14. ¹³C NMR spectrum of **C22** in CDCl₃.
Fig. S15. HRMS spectrum of **C22** (ESI, positive). Top: obsd. Bottom: sim.
Fig. S16. ¹H NMR spectrum of **C22i** in CDCl₃.
Fig. S17. ¹³C NMR spectrum of **C22i** in CDCl₃.
Fig. S18. HRMS spectrum of **C22i** (ESI, positive). Top: obsd. Bottom: sim.
Fig. S19. ¹H NMR spectrum of **Flu-d₄** in CDCl₃.
Fig. S20. ¹³C NMR spectrum of **Flu-d₄** in CDCl₃.
Fig. S21. HRMS spectrum of **Flu-d₄** (ESI, positive). Top: obsd. Bottom: sim.
Fig. S22. ¹H NMR spectrum of **BrFluBr-d₃** in CDCl₃.
Fig. S23. ¹³C NMR spectrum of **BrFluBr-d₃** in CDCl₃.
Fig. S24. HRMS spectrum of **BrFluBr-d₃** (ESI, positive). Top: obsd. Bottom: sim.
Fig. S25. ¹H NMR spectrum of **C10FluC10-d₃** in CDCl₃.
Fig. S26. ¹³C NMR spectrum of **C10FluC10-d₃** in CDCl₃.
Fig. S27. HRMS spectrum of **C10FluC10-d₃** (ESI, positive). Top: obsd. Bottom: sim.
Fig. S28. ¹H NMR spectrum of **C18-d₃** in CDCl₃.
Fig. S29. ¹³C NMR spectrum of **C18-d₃** in CDCl₃.
Fig. S30. HRMS spectrum of **C18-d₃** (ESI, positive). Top: obsd. Bottom: sim.
Fig. S31. ¹H NMR spectrum of **C12FluC12-d₃** in CDCl₃.
Fig. S32. ¹³C NMR spectrum of **C12FluC12-d₃** in CDCl₃.
Fig. S33. HRMS spectrum of **C12FluC12-d₃** (ESI, positive). Top: obsd. Bottom: sim.
Fig. S34. ¹H NMR spectrum of **C22-d₃** in CDCl₃.
Fig. S35. ¹³C NMR spectrum of **C22-d₃** in CDCl₃.
Fig. S36. HRMS spectrum of **C22-d₃** (ESI, positive). Top: obsd. Bottom: sim.

2. Appended Data of X-ray Crystallography

Table S1. Crystal Data

- Fig. S37.** An ORTEP drawing (30% thermal ellipsoids) of molecular structure of **C18** determined by X-ray crystallography.
Fig. S38. An ORTEP drawing (30% thermal ellipsoids) of molecular structure of **C22•2EtOH** determined by X-ray crystallography.
Fig. S39. An ORTEP drawing (30% thermal ellipsoids) of molecular structure of **Flu** determined by X-ray crystallography.
Fig. S40. An ORTEP drawing (30% thermal ellipsoids) of molecular structure of **TMS** determined by X-ray crystallography.

3. Appended Data of Fluorescence Measurements

- Fig. S41.** Fluorescence life-time measurements for fluorenes in hexane: (a) **C18**, (b) **C22**, (c) **TMS**, and (d) **Flu**.
Fig. S42. Fluorescence life-time measurements for fluorenes in solid-states: (a) **C18**, (b) **C22**, (c) **TMS**, and (d) **Flu**.

4. Appended Data of Solid-state ²H NMR Study

- Figure S43.** Inversion-recovery ²H NMR spectroscopy data (300 K) and single exponential fit of (a) **C18-d₃** and (b) **C22-d₃**.

1. Copies of NMR and HRMS Spectra for New Compounds

a. Spectra of C10FluC10

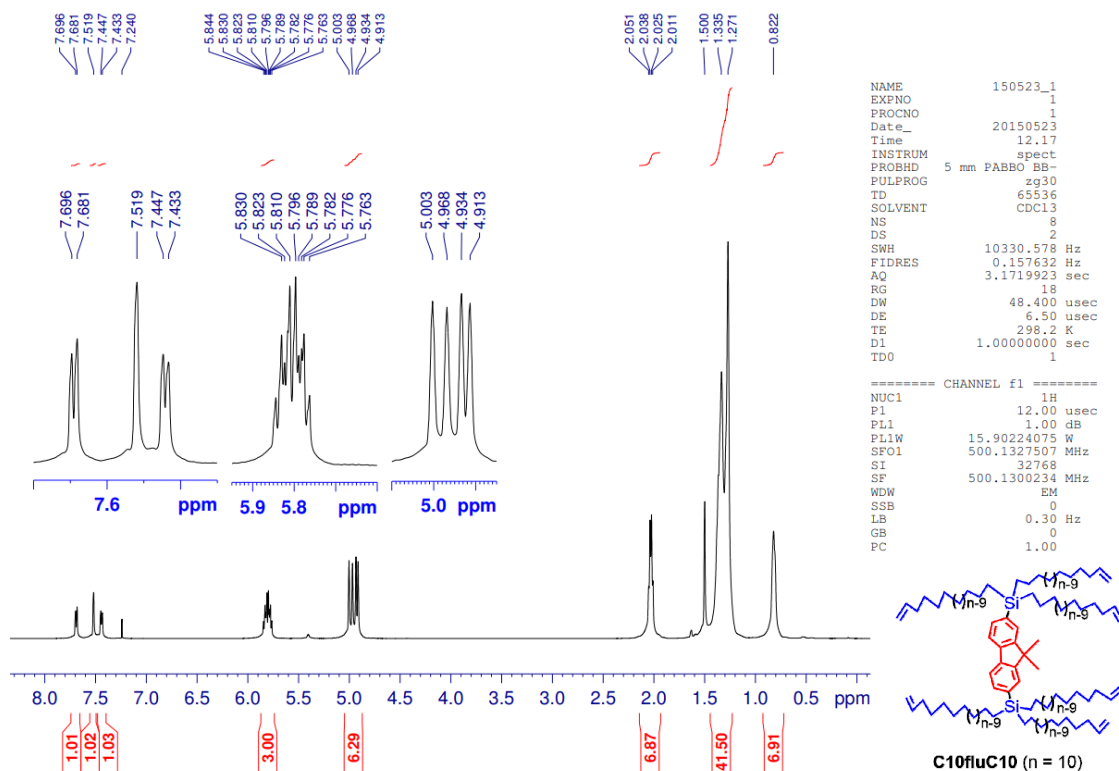


Fig. S1. ¹H NMR spectrum of C10FluC10 in CDCl₃.

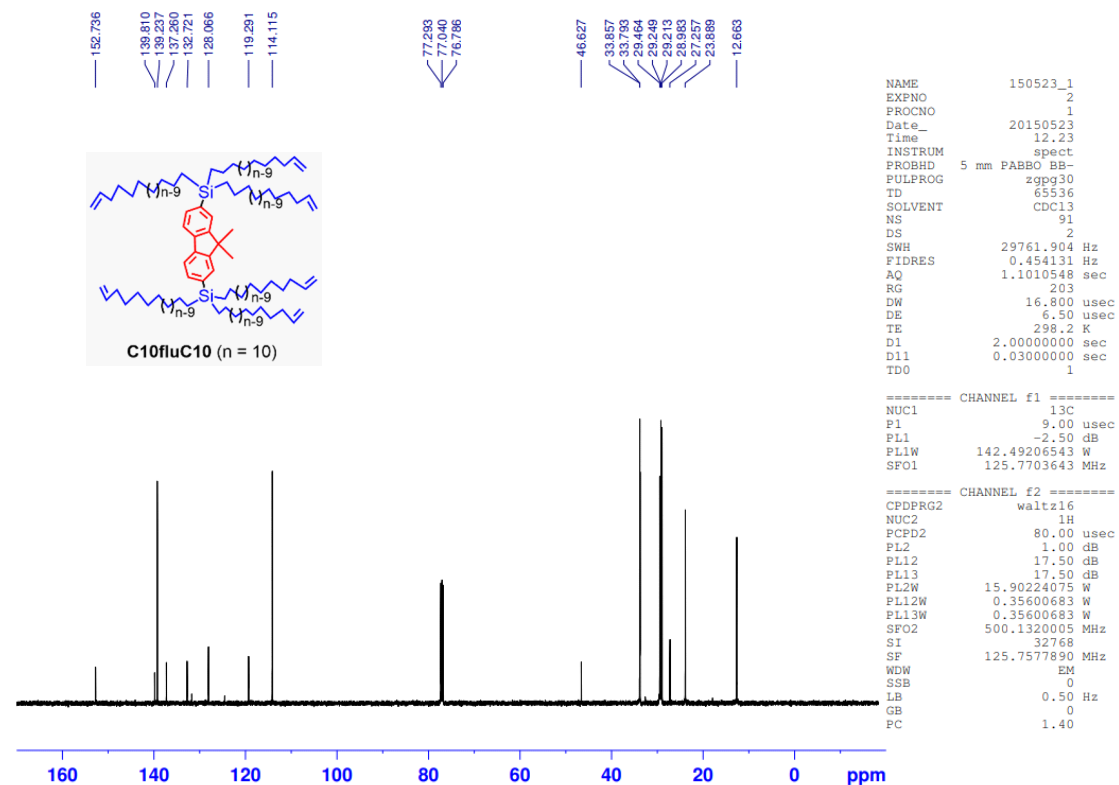


Fig. S2. ¹³C NMR spectrum of C10FluC10 in CDCl₃.

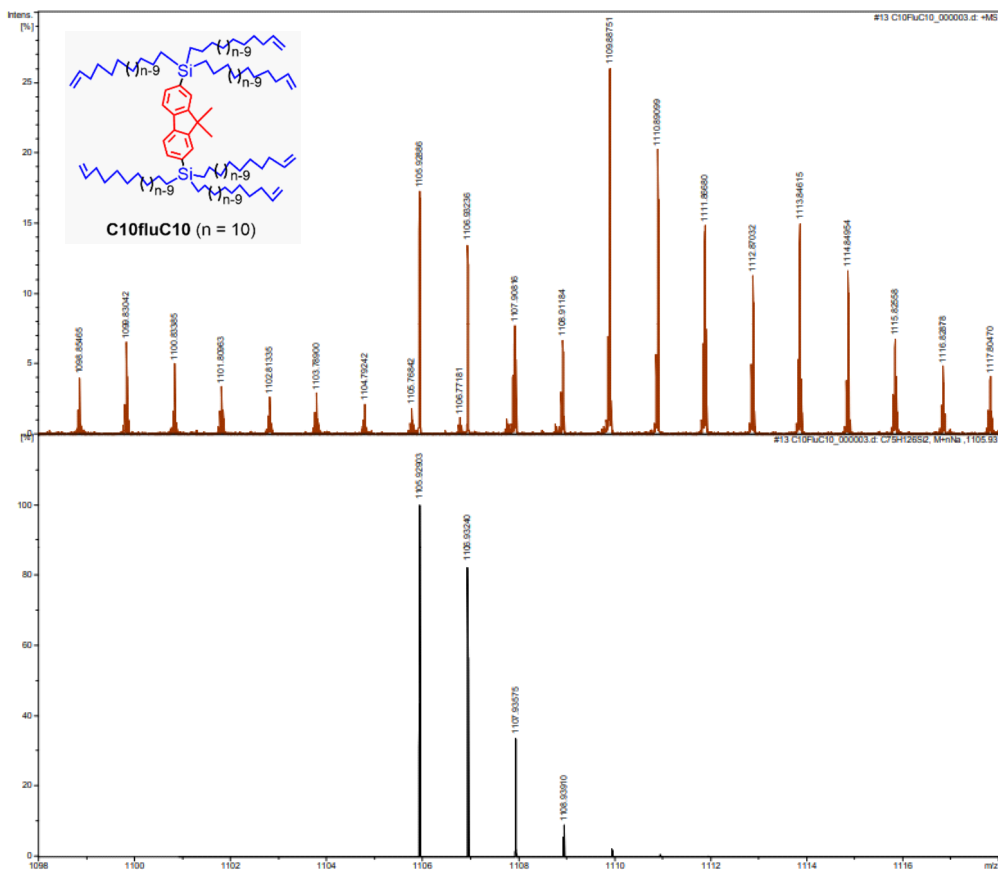


Fig. S3. HRMS spectrum of C10FluC10 (ESI, positive). Top: obsd. Bottom: sim.

b. Spectra of C12FluC12

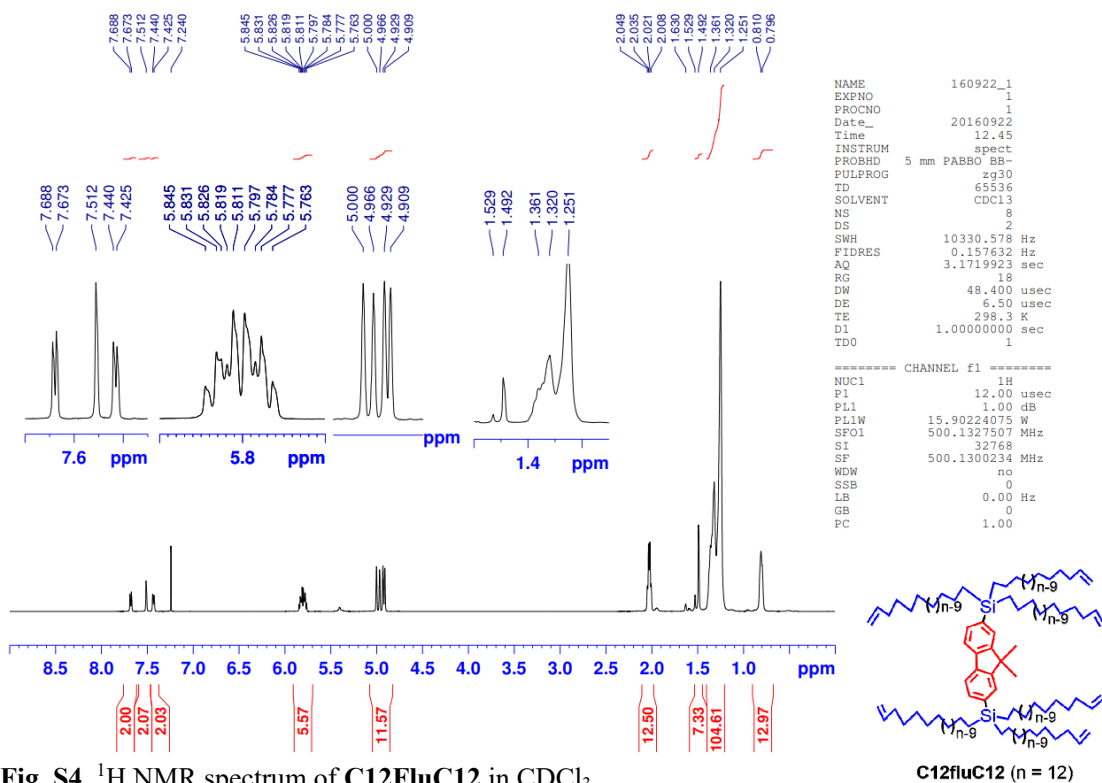


Fig. S4. ¹H NMR spectrum of C12FluC12 in CDCl₃.

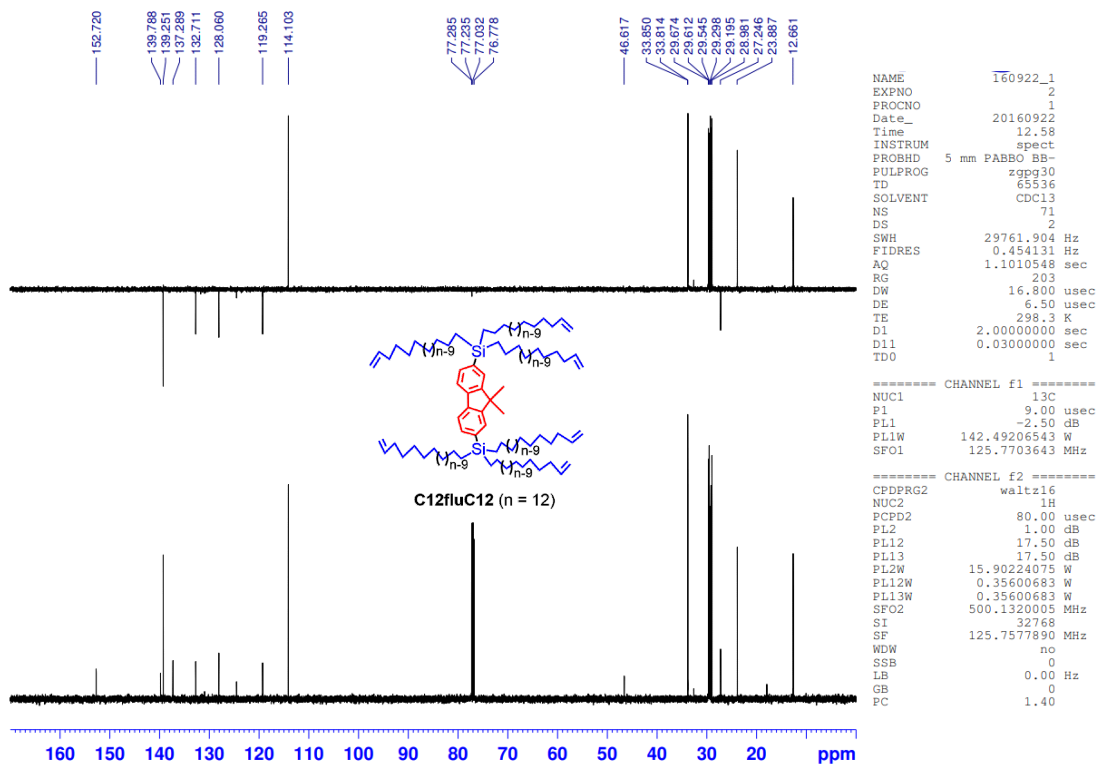


Fig. S5. ^{13}C NMR spectrum of C12FluC12 in CDCl_3 .

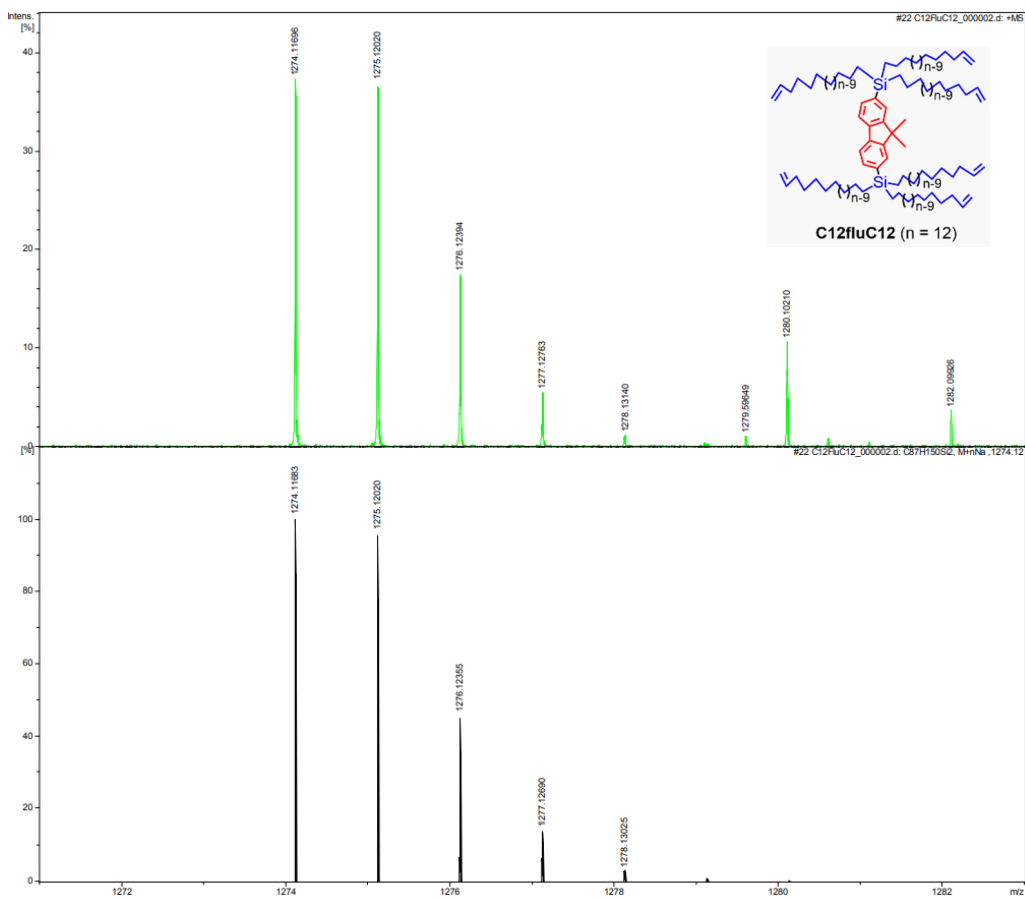


Fig. S6. HRMS spectrum of C12FluC12 (ESI, positive). Top: obsd. Bottom: sim.

c. Spectra of C18

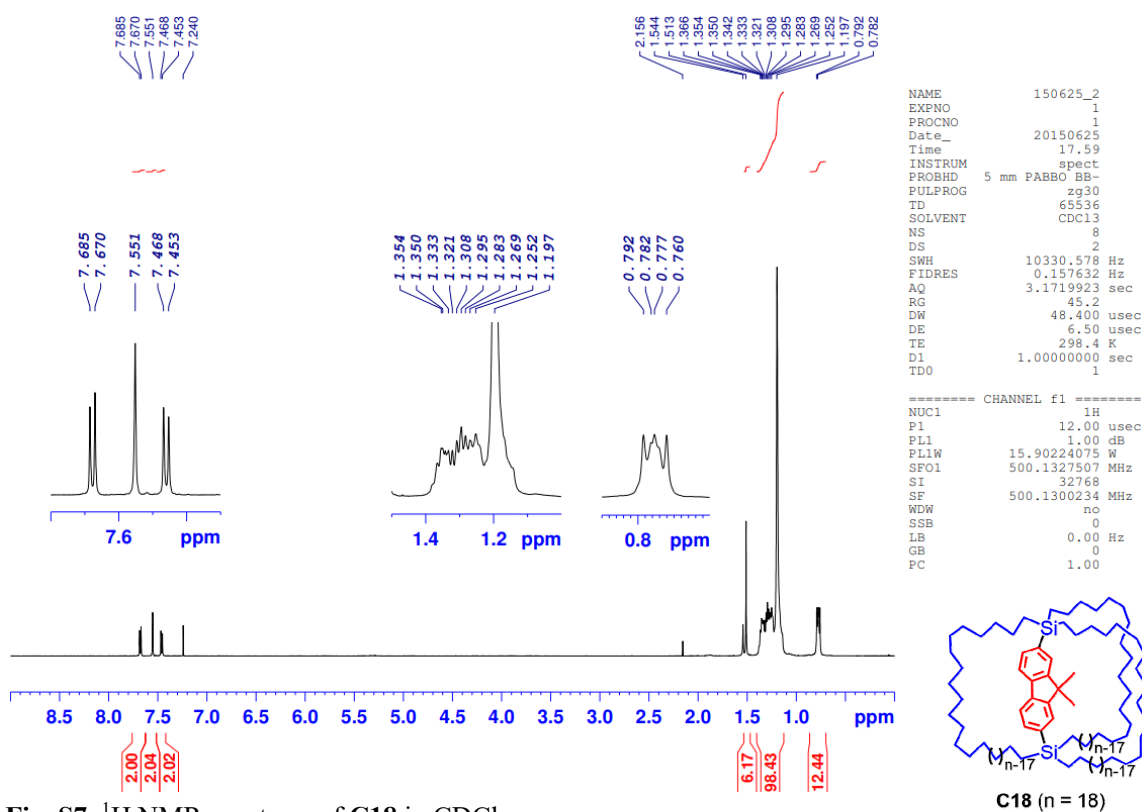


Fig. S7. ¹H NMR spectrum of C18 in CDCl₃.

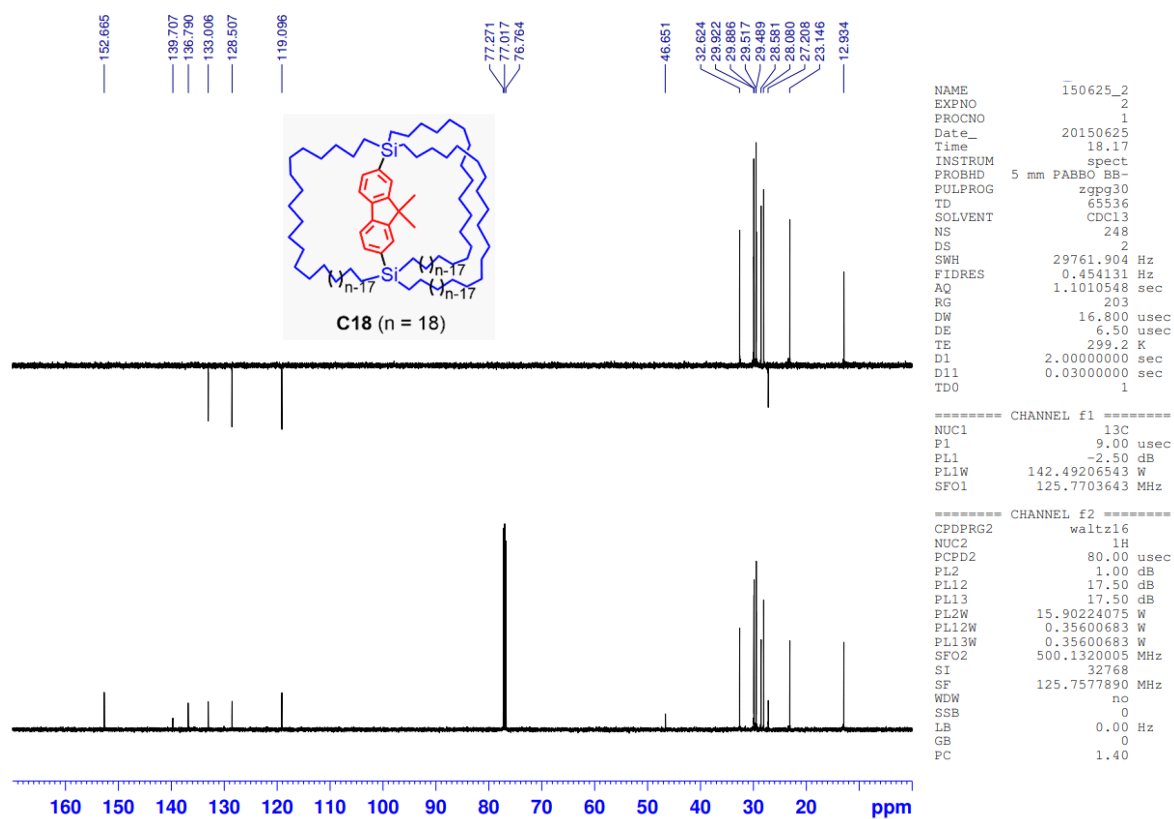


Fig. S8. ¹³C NMR spectrum of C18 in CDCl₃.

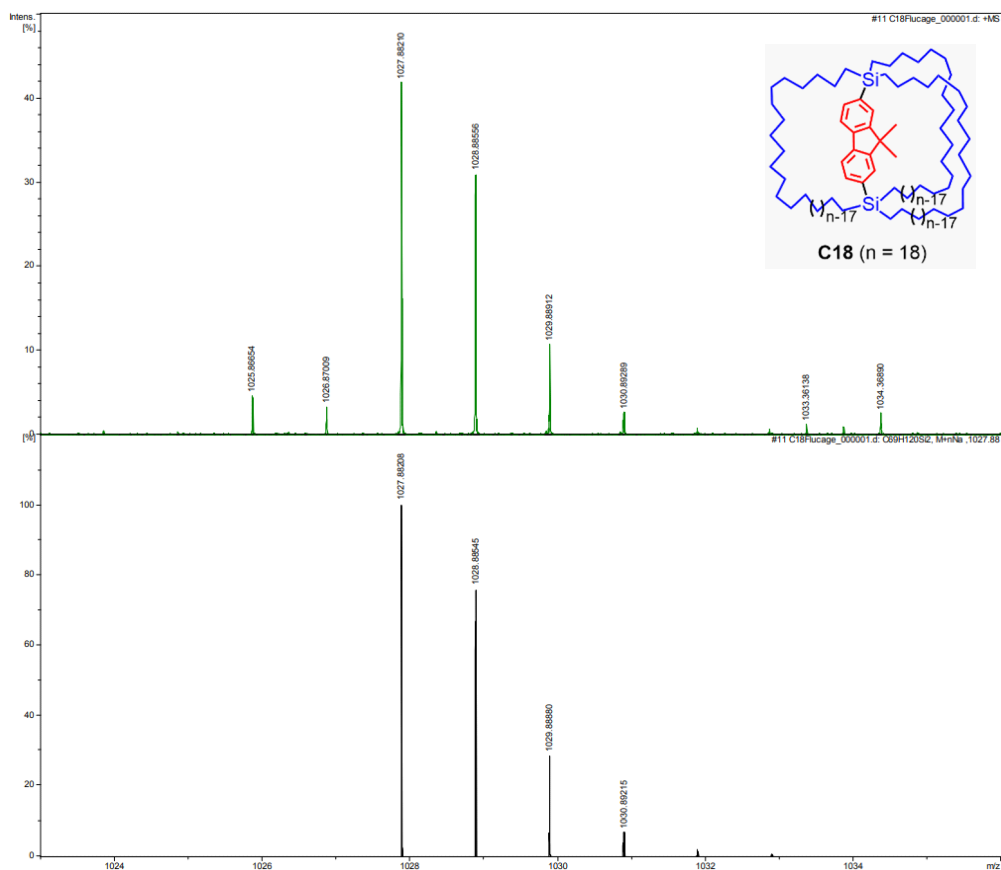


Fig. S9. HRMS spectrum of C18 (ESI, positive). Top: obsd. Bottom: sim.

d. Spectra of C18i

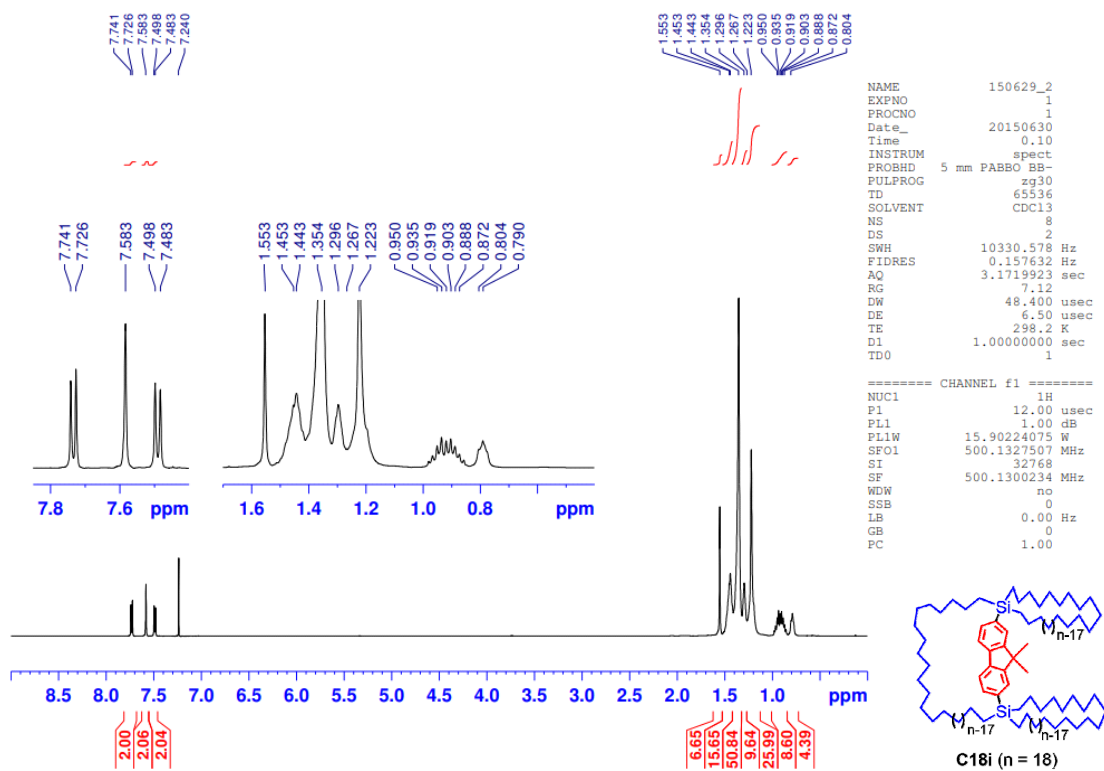


Fig. S10. ¹H NMR spectrum of C18i in CDCl₃.

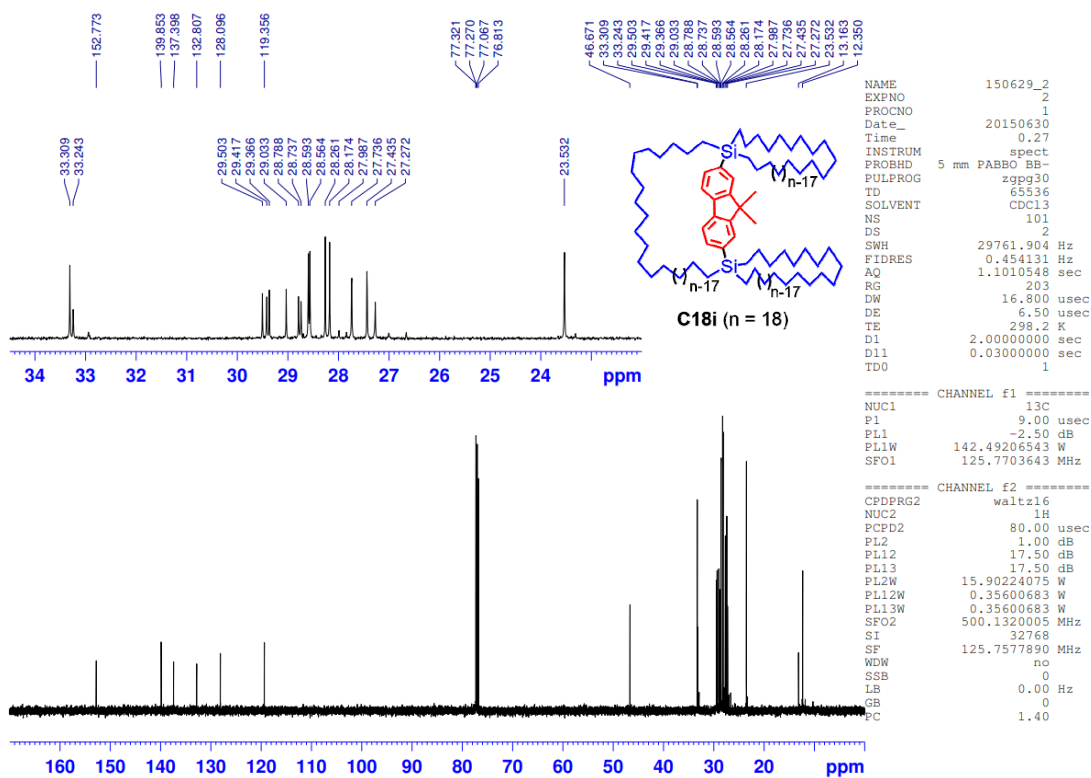


Fig. S11. ^{13}C NMR spectrum of **C18i** in CDCl_3 .

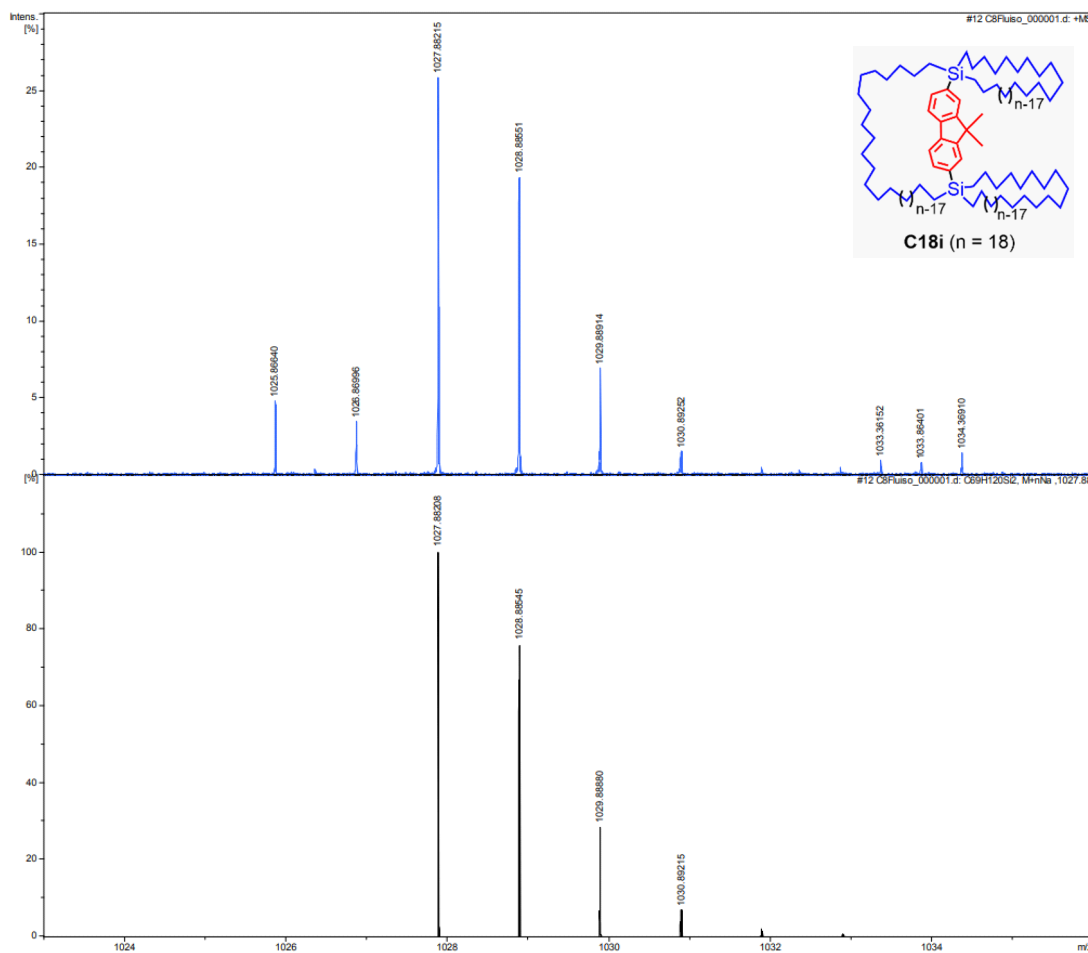


Fig. S12. HRMS spectrum of **C18i** (ESI, positive). Top: obsd. Bottom: sim.

e. Spectra of C22

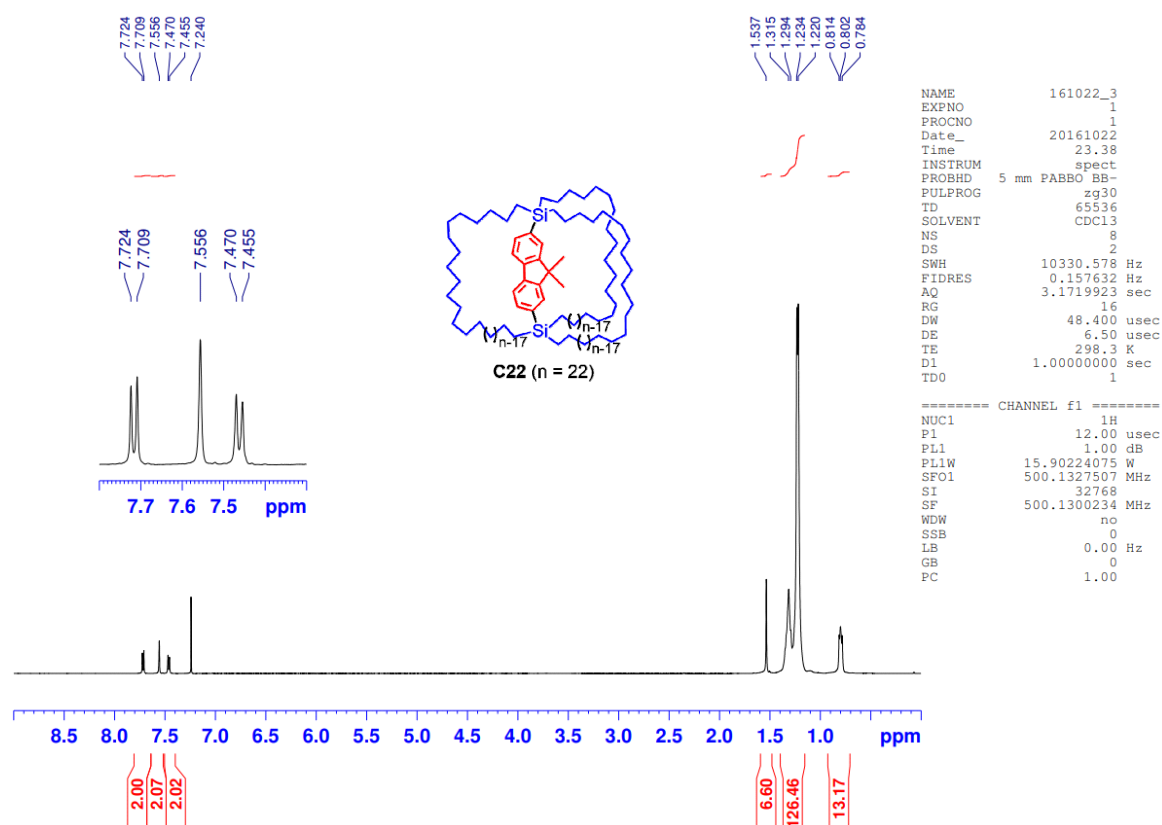


Fig. S13. ¹H NMR spectrum of C22 in CDCl₃.

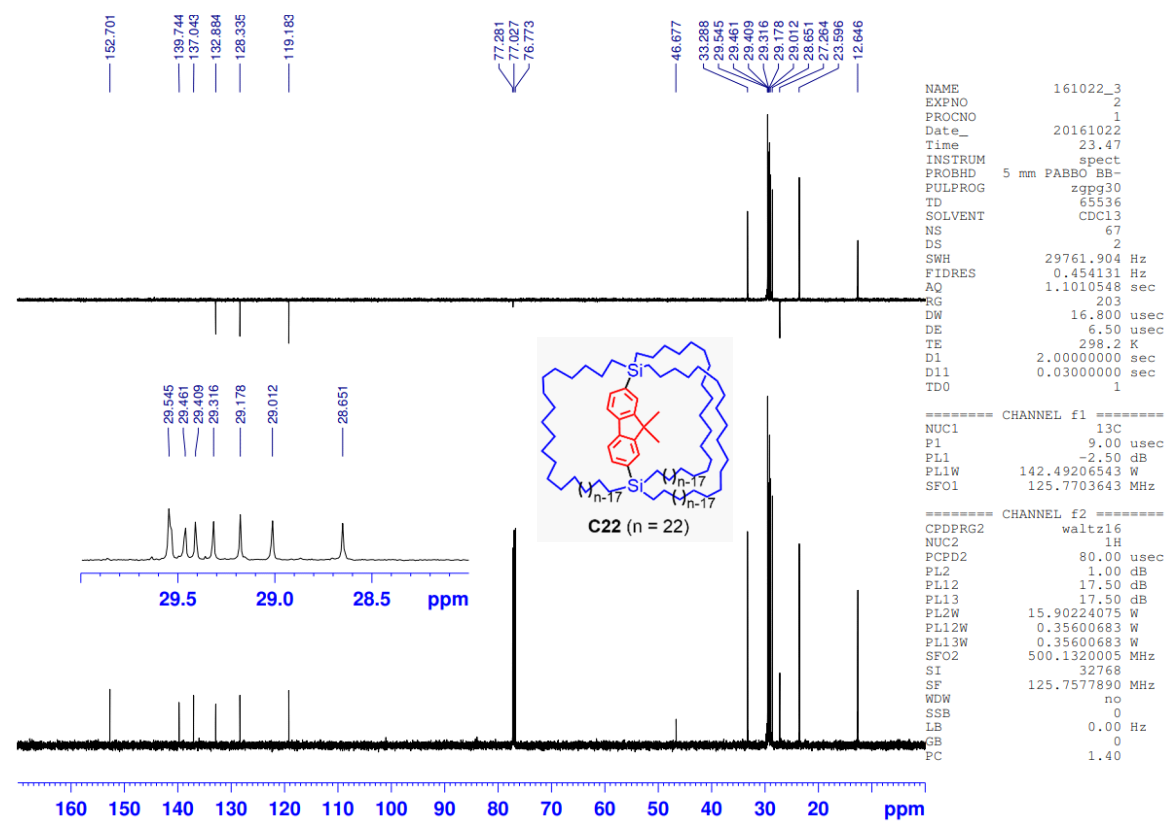


Fig. S14. ¹³C NMR spectrum of C22 in CDCl₃.

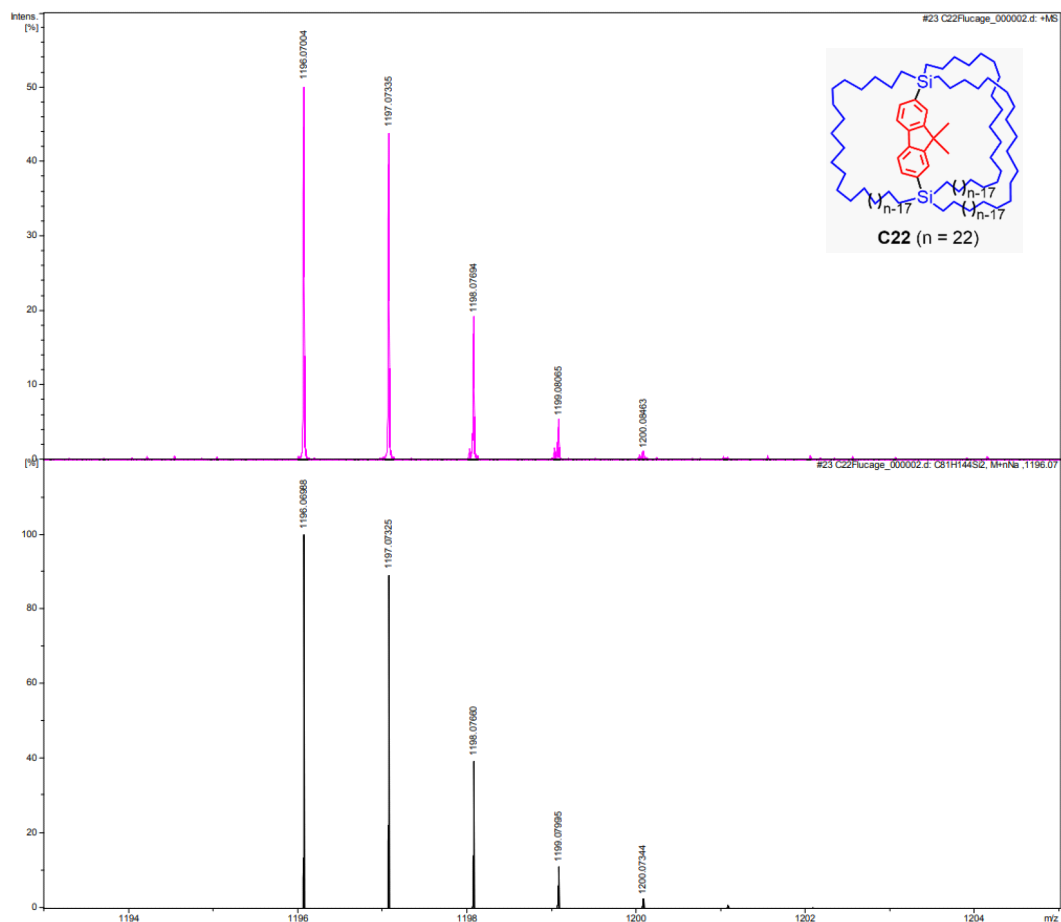


Fig. S15. HRMS spectrum of C22 (ESI, positive). Top: obsd. Bottom: sim.

f. Spectra of C22i

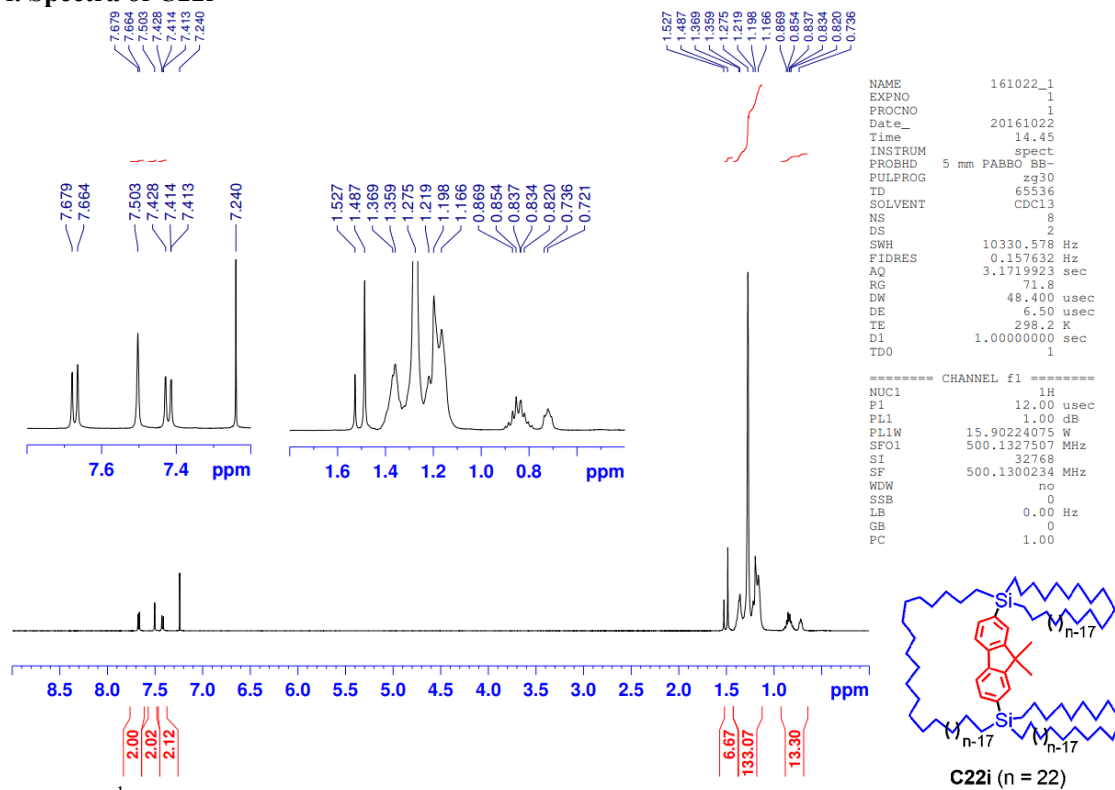


Fig. S16. ¹H NMR spectrum of C22i in CDCl₃.

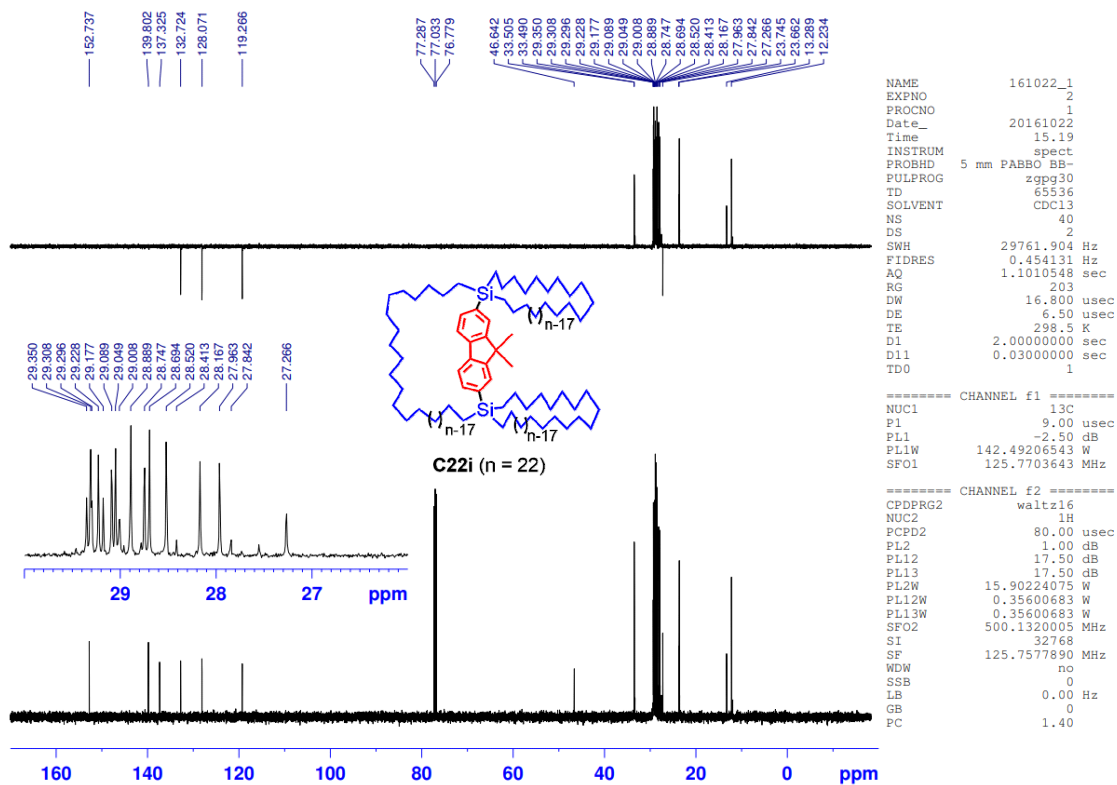


Fig. S17. ¹³C NMR spectrum of C22i in CDCl₃.

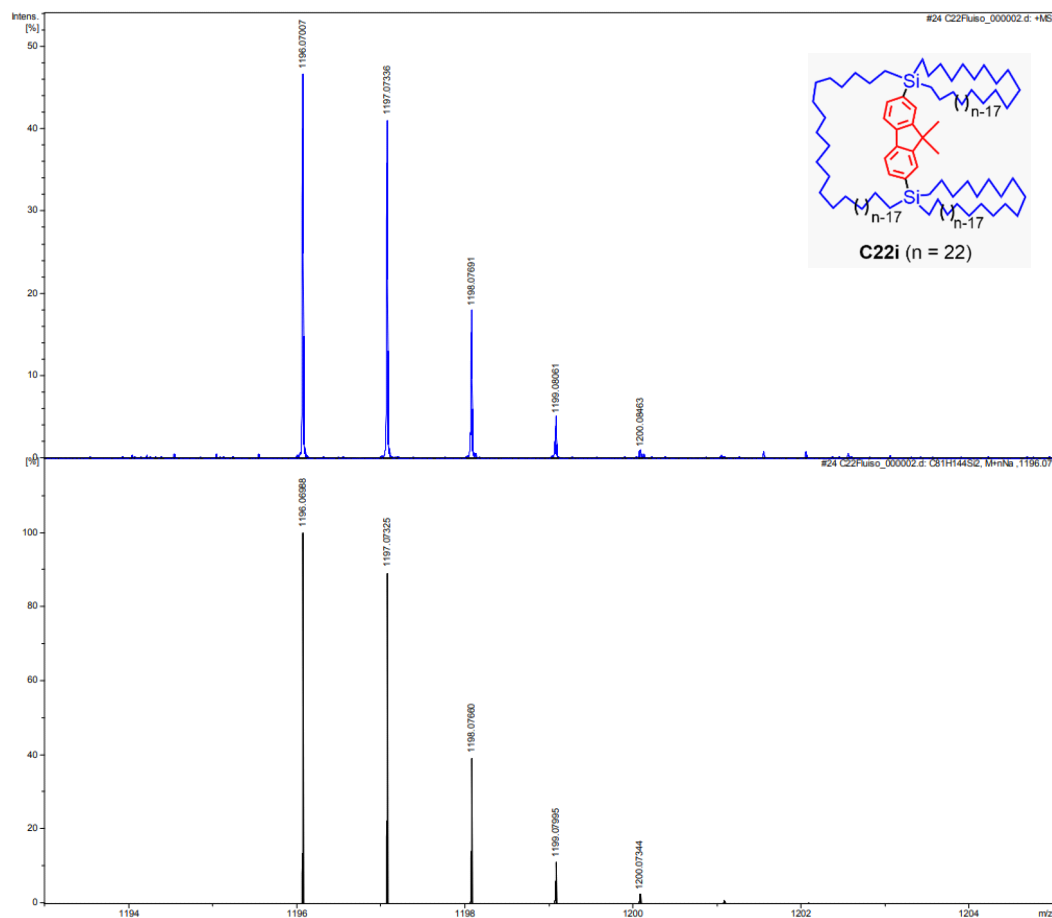


Fig. S18. HRMS spectrum of C22i (ESI, positive). Top: obsd. Bottom: sim.

g. Spectra of Flu-*d*₄

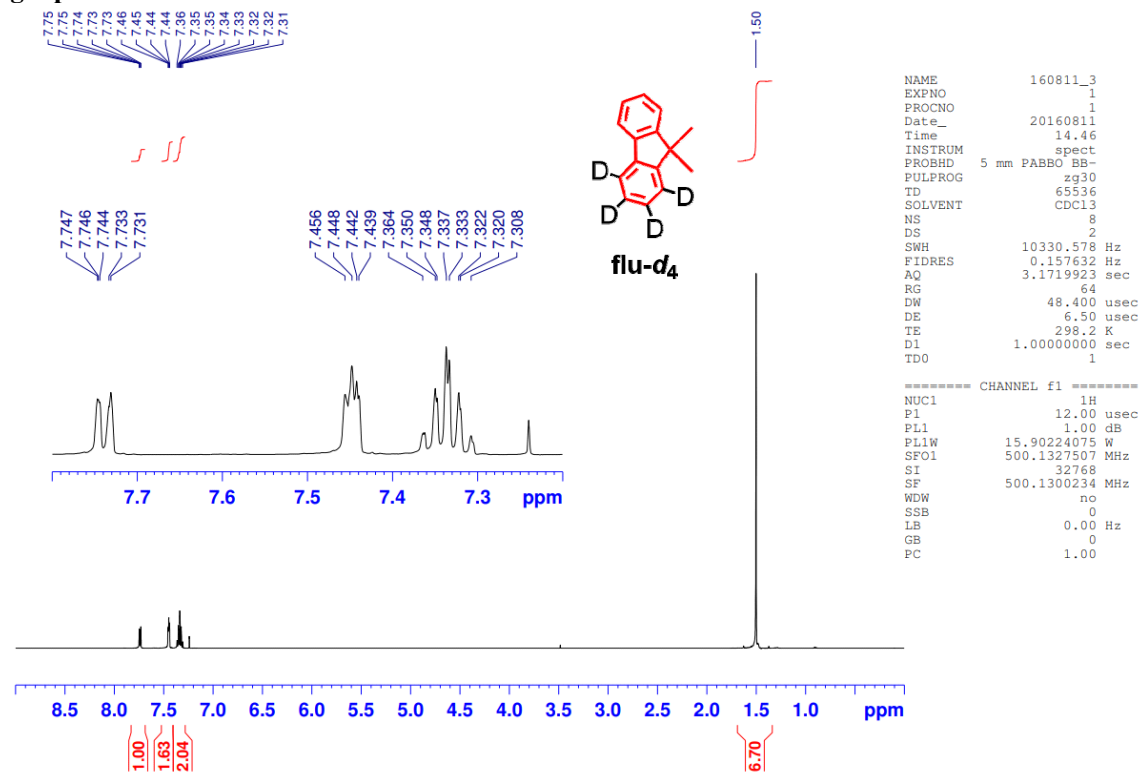


Fig. S19. ¹H NMR spectrum of Flu-*d*₄ in CDCl₃.

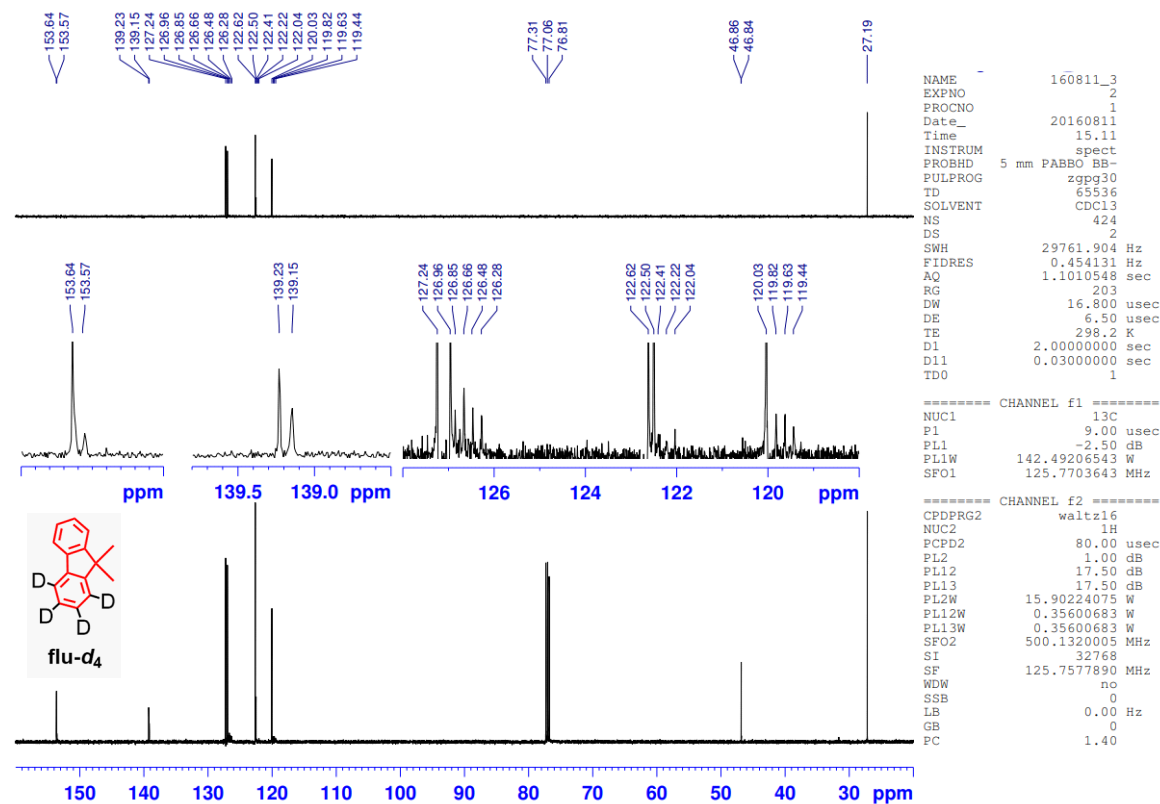


Fig. S20. ¹³C NMR spectrum of Flu-*d*₄ in CDCl₃.

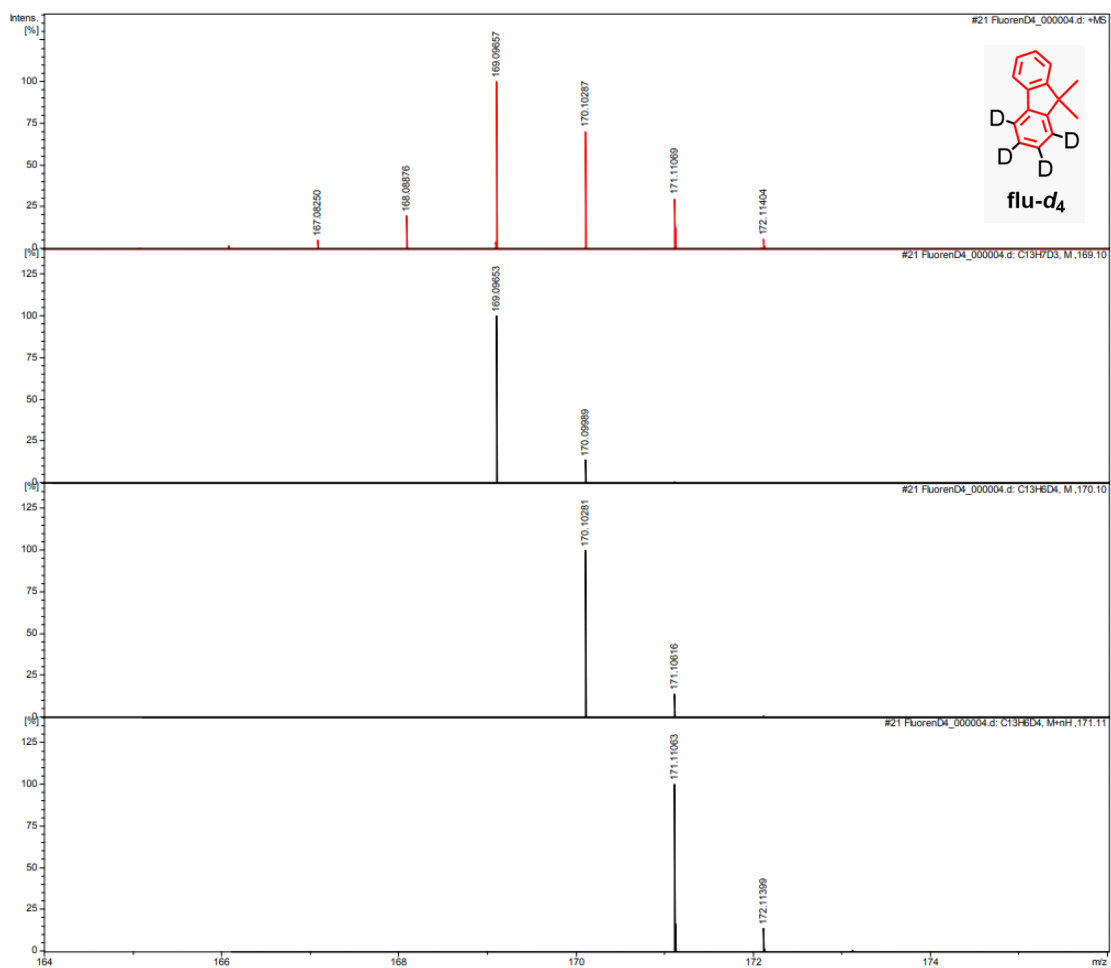


Fig. S21. HRMS spectrum of Flu-d₄ (ESI, positive). Top: obsd. Bottom: sim.

h. Spectra of BrFluBr-d₃

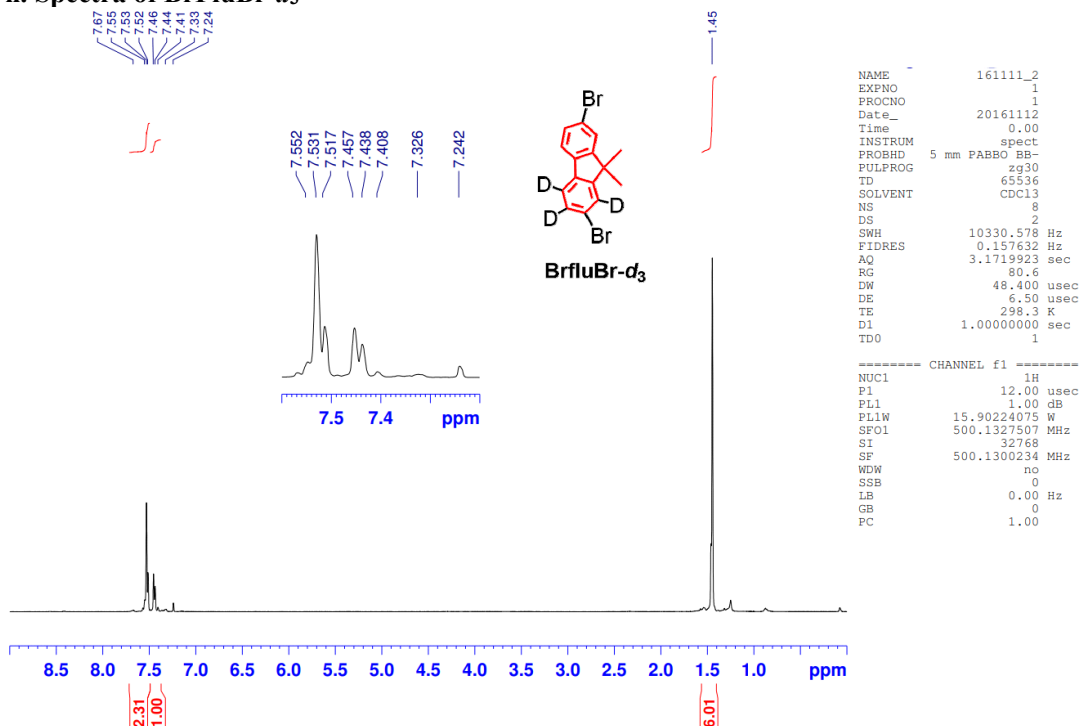


Fig. S22. ¹H NMR spectrum of BrFluBr-d₃ in CDCl₃.

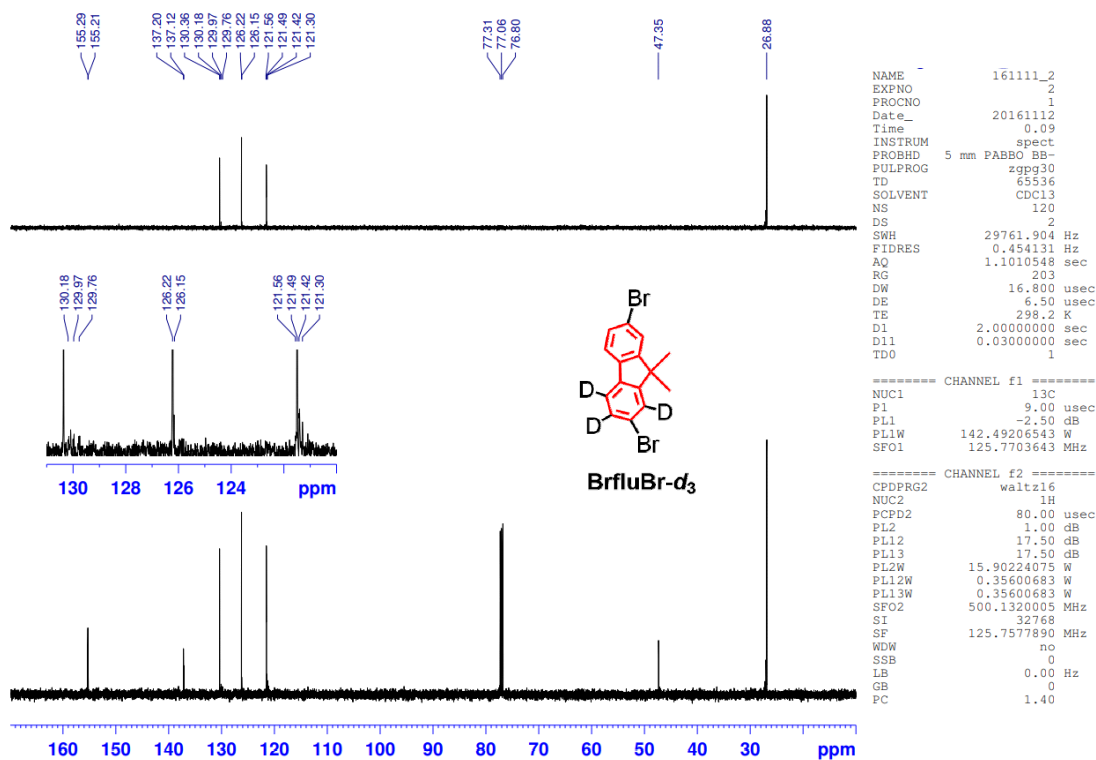


Fig. S23. ^{13}C NMR spectrum of **BrFluBr- d_3** in CDCl_3 .

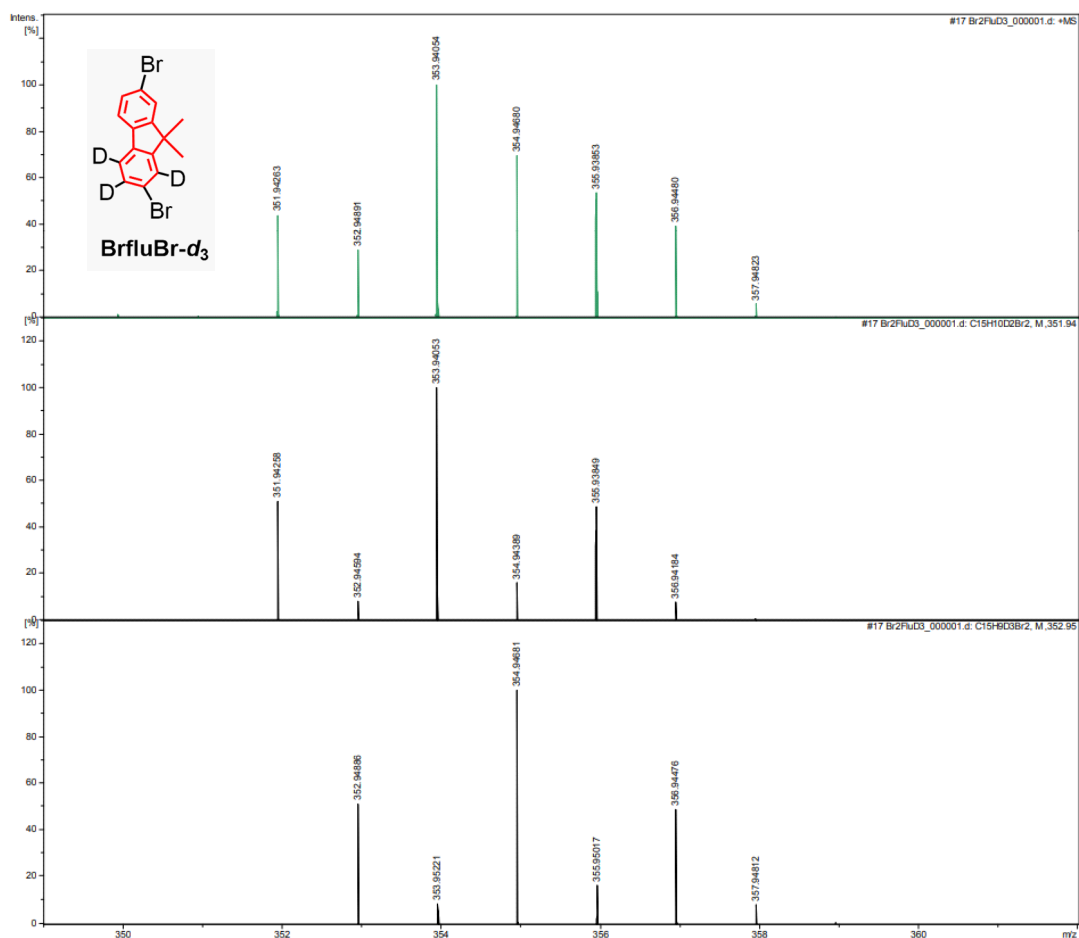


Fig. S24. HRMS spectrum of **BrFluBr- d_3** (ESI, positive). Top: obsd. Bottom: sim.

i. Spectra of C10FluC10-d₃

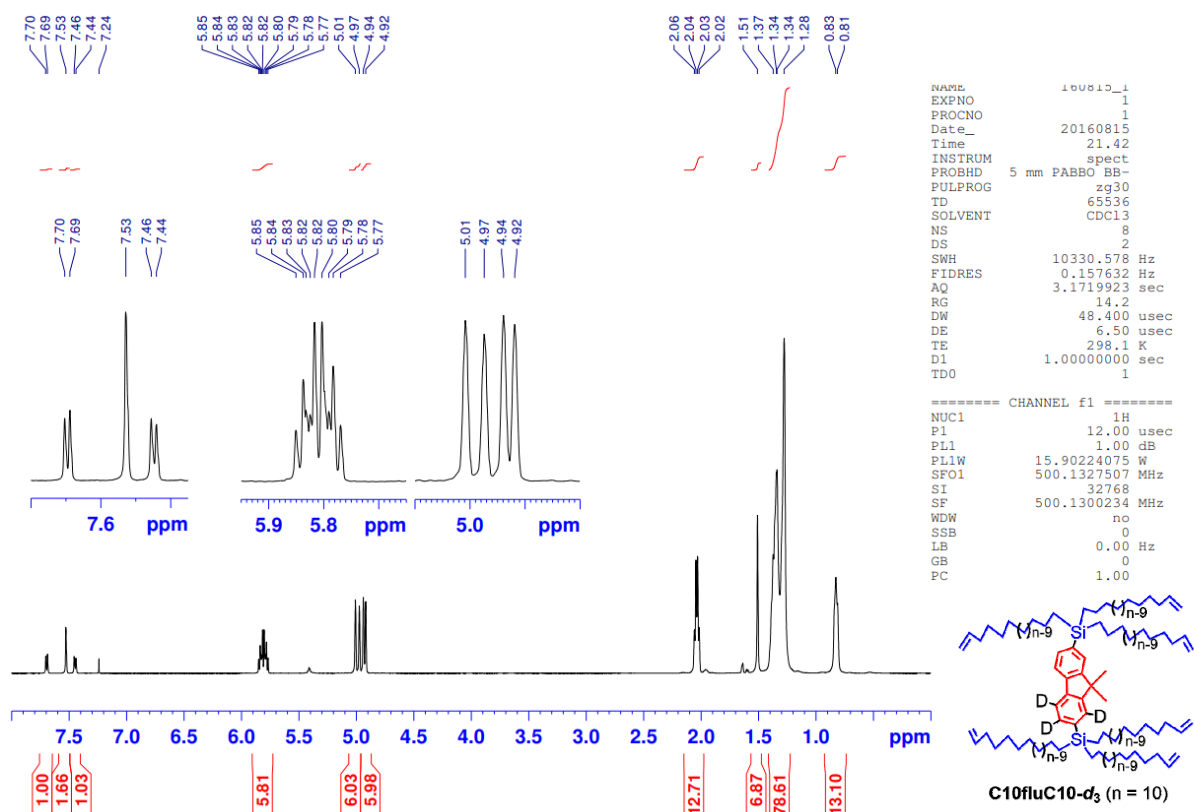


Fig. S25. ¹H NMR spectrum of C10FluC10-d₃ in CDCl₃.

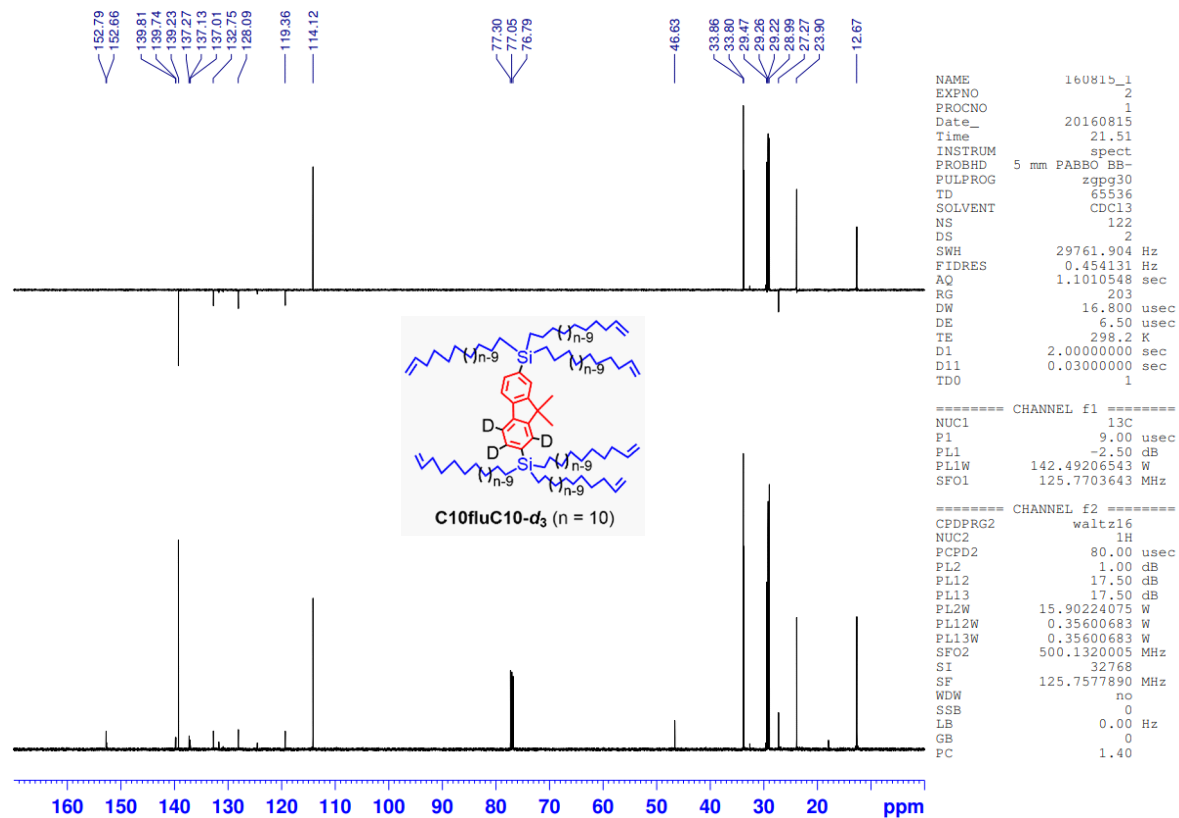


Fig. S26. ¹³C NMR spectrum of C10FluC10-d₃ in CDCl₃.

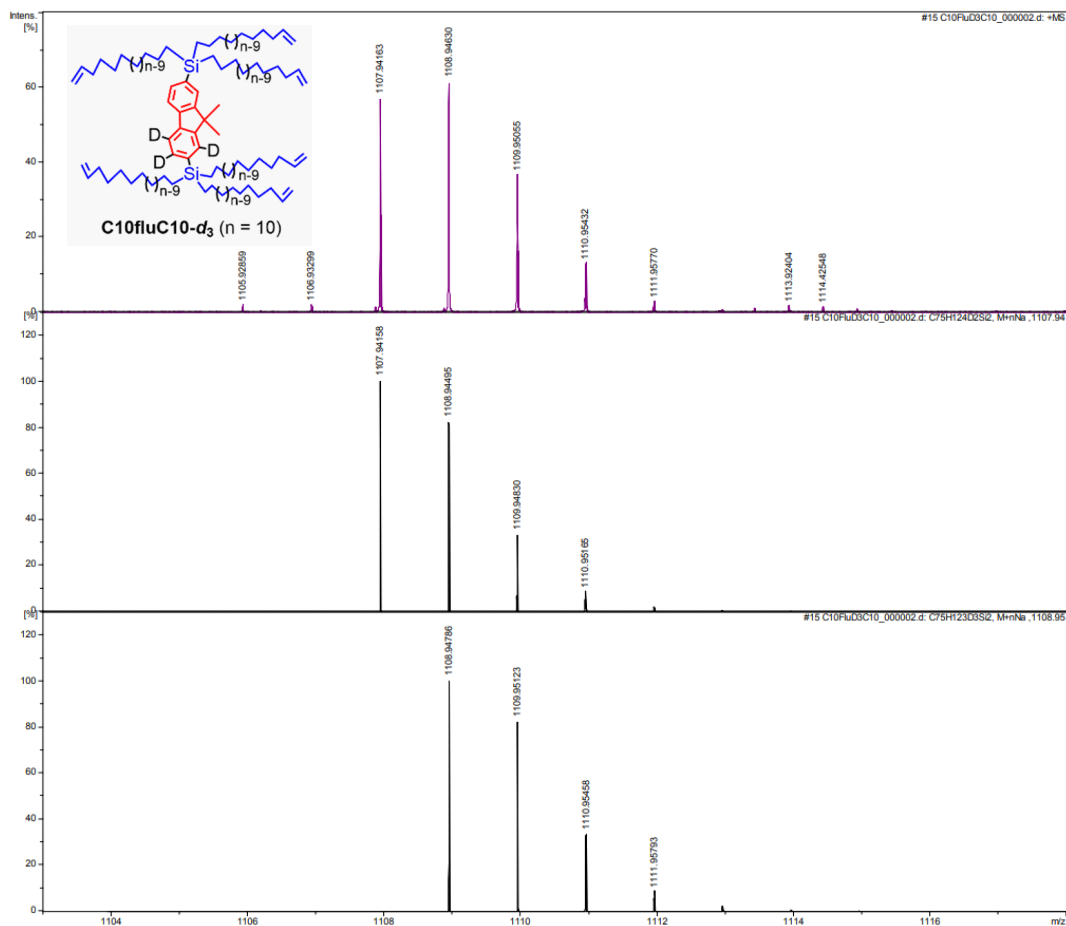


Fig. S27. HRMS spectrum of **C10FluC10-d₃** (ESI, positive). Top: obsd. Bottom: sim.

k. Spectra of **C18-d₃**

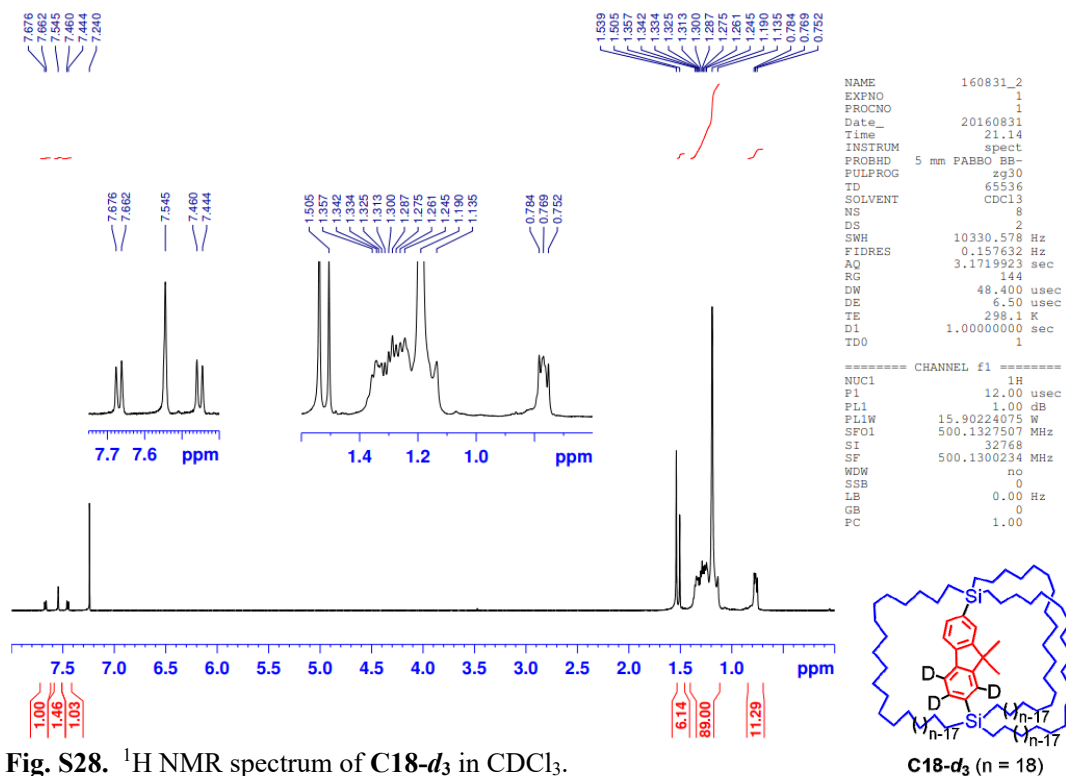


Fig. S28. ¹H NMR spectrum of **C18-d₃** in CDCl₃.

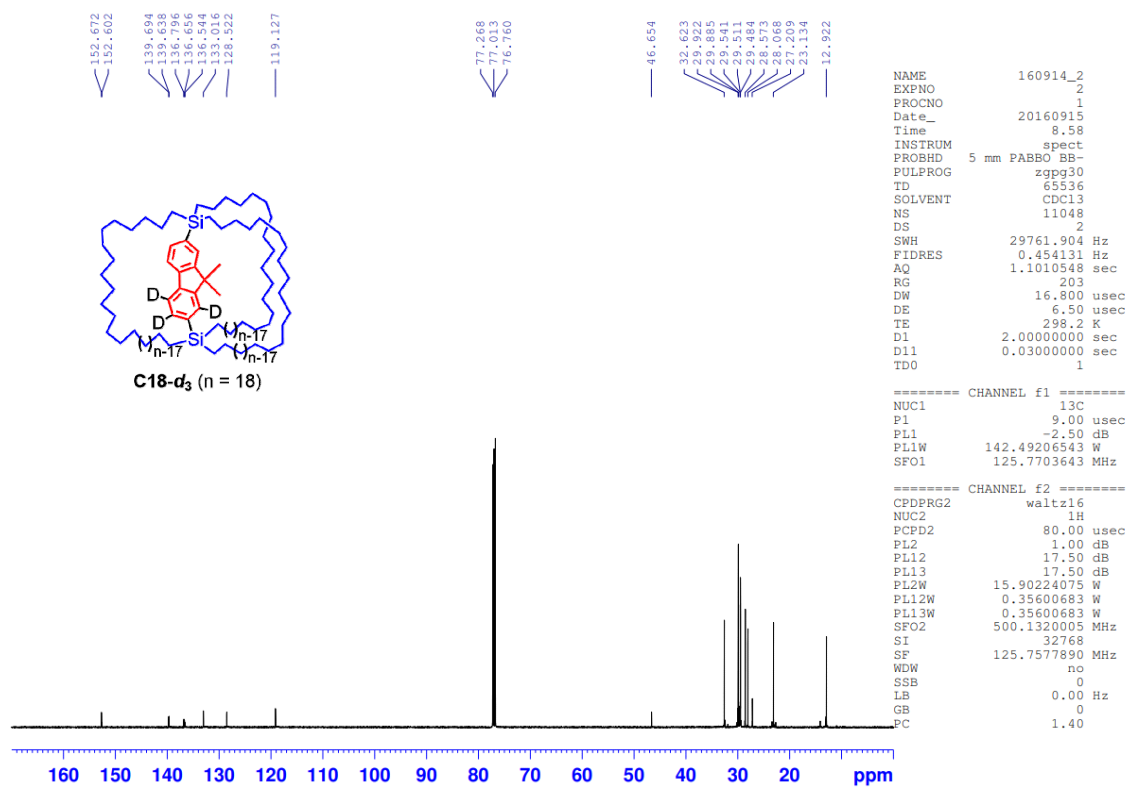


Fig. S29. ^{13}C NMR spectrum of C18-d_3 in CDCl_3 .

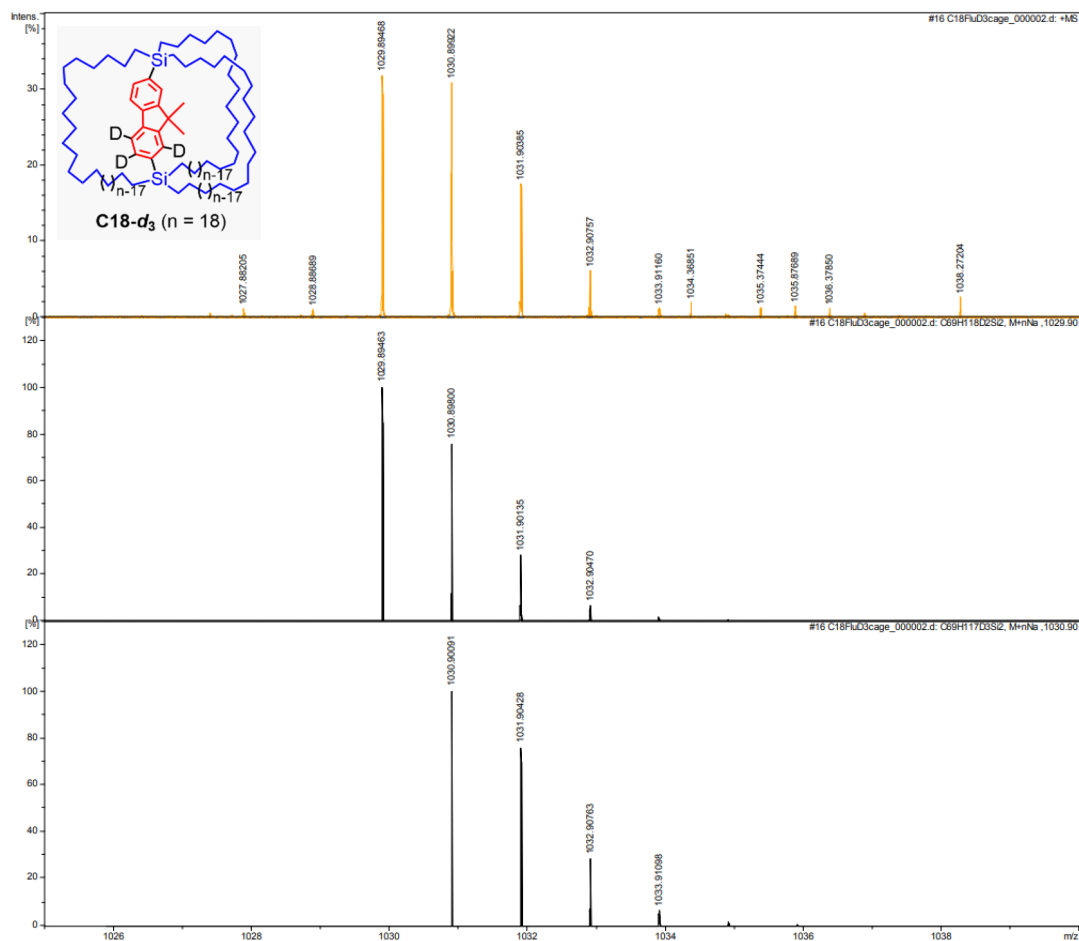


Fig. S30. HRMS spectrum of C18-d_3 (ESI, positive). Top: obsd. Bottom: sim.

j. Spectra of C12FluC12-d₃

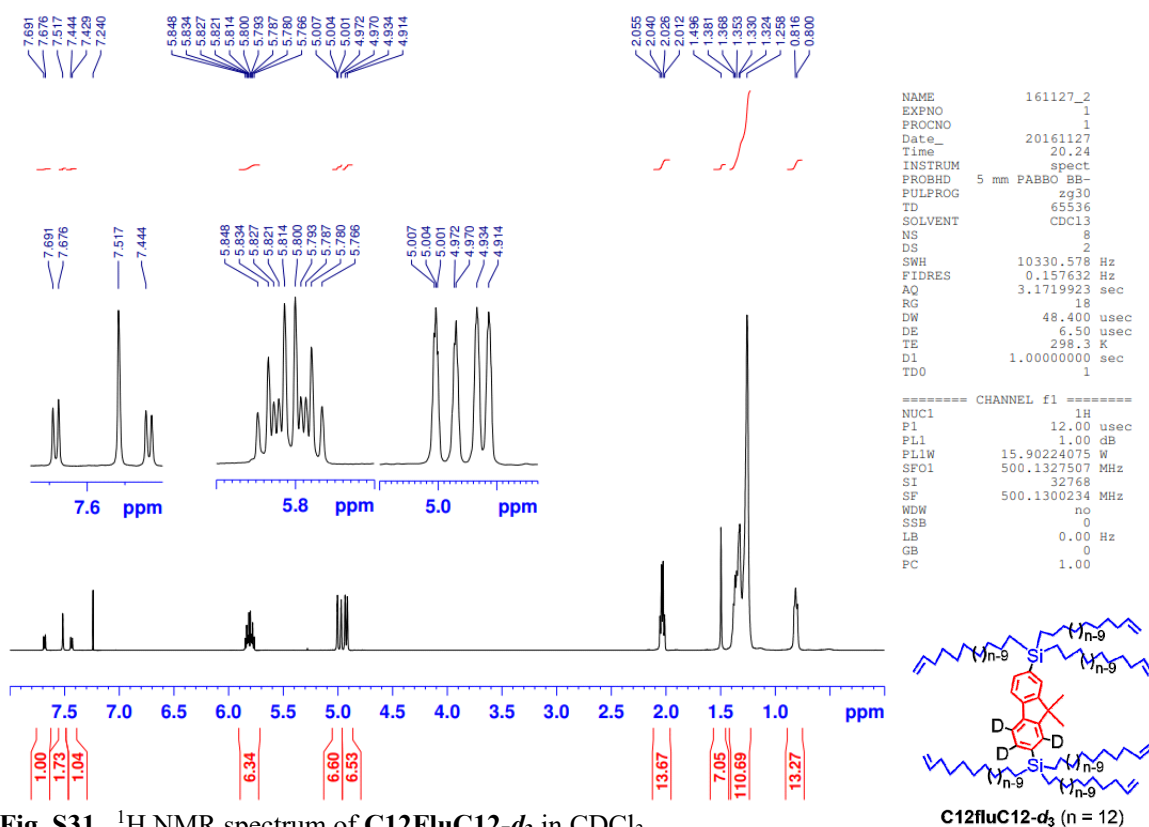


Fig. S31. ¹H NMR spectrum of C12FluC12-d₃ in CDCl₃.

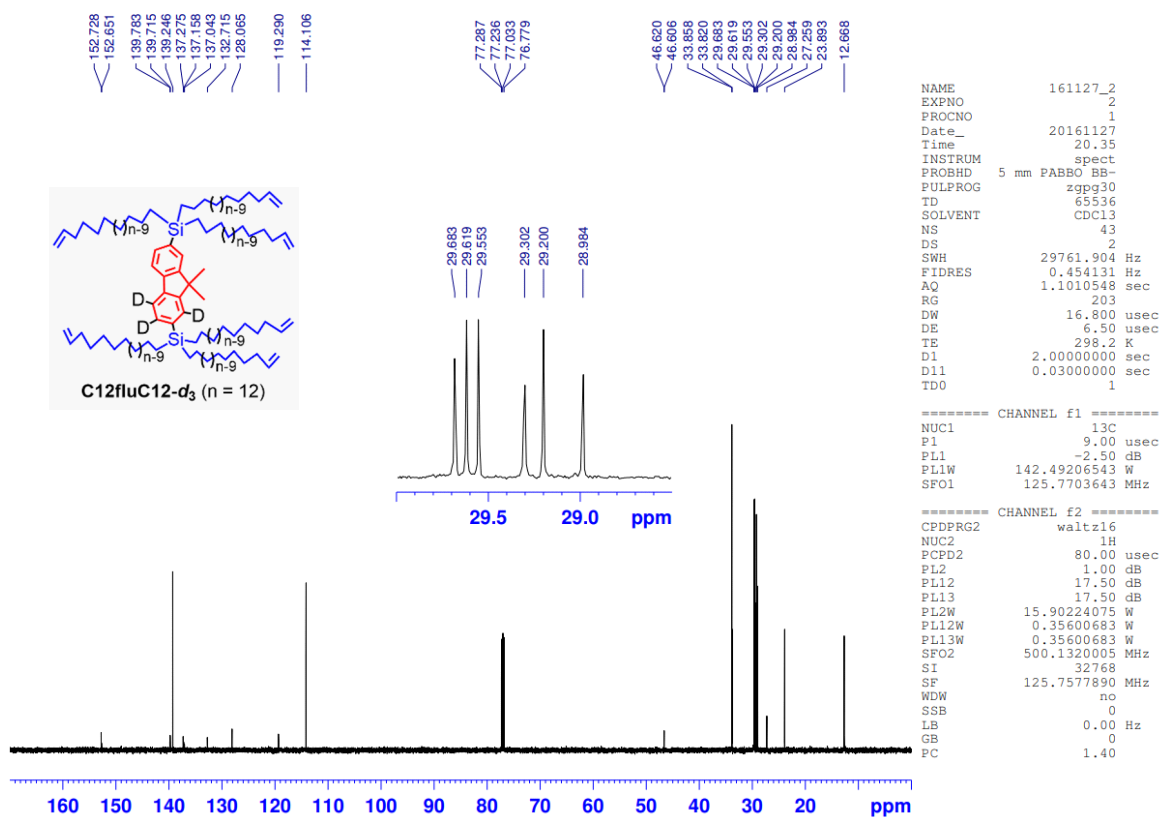


Fig. S32. ¹³C NMR spectrum of C12FluC12-d₃ in CDCl₃.

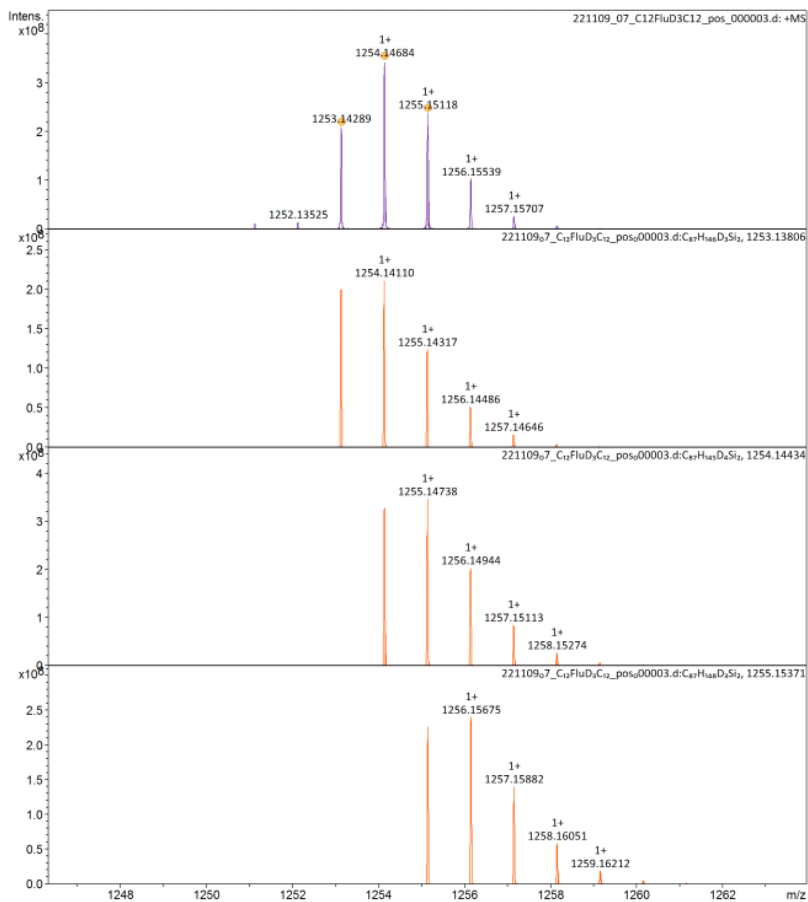


Fig. S33. HRMS spectrum of C12FluC12- d_3 (ESI, positive). Top: obsd. Bottom: sim.

I. Spectra of C22- d_3

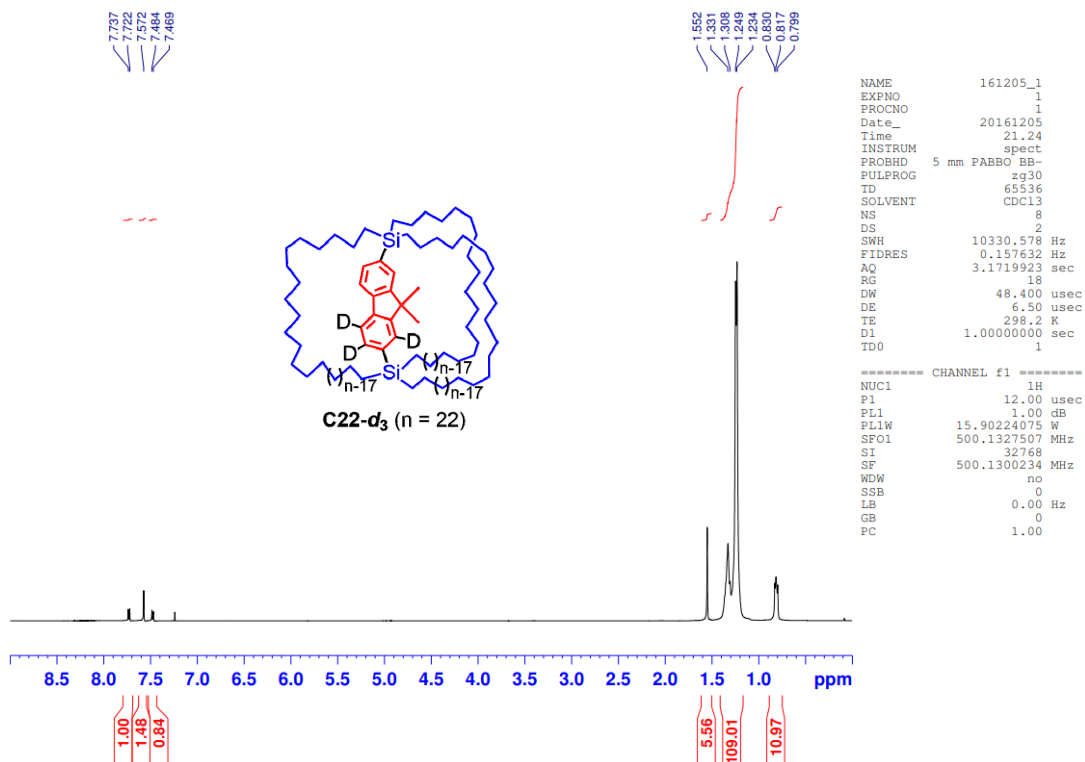


Fig. S34. ^1H NMR spectrum of C22- d_3 in CDCl_3 .

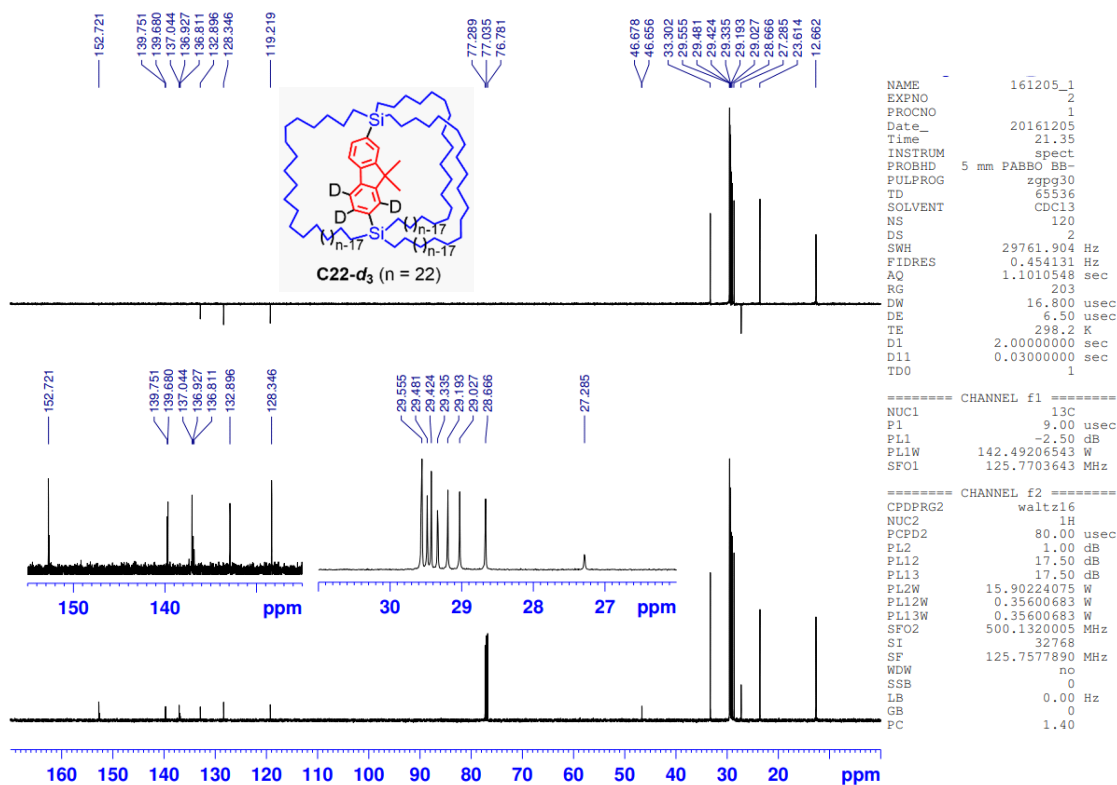


Fig. S35. ^{13}C NMR spectrum of C22-d_3 in CDCl_3 .

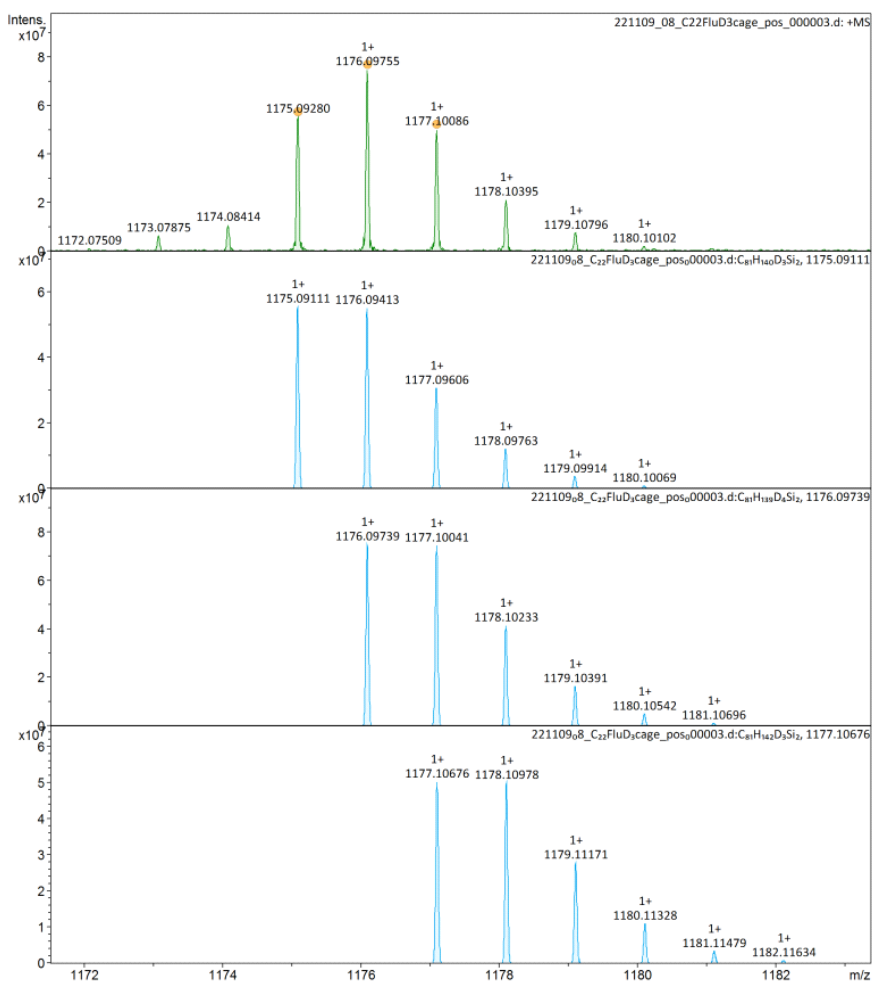


Fig. S36. HRMS spectrum of C22-d_3 (ESI, positive). Top: obsd. Bottom: sim.

2. Appended Data of X-ray Crystallography

2-1. Crystal Data

Table S1. Crystal Data

| Compound | C18 | C22•2EtOH | Flu | TMS | |
|--------------------------------------|---|---|---|---|---------------------------|
| CCDC # | 2223164 | 2223165 | 2239859 | 2239860 | |
| Empirical formula | C ₆₉ H ₁₂₀ Si ₂ | C ₈₁ H ₁₄₄ Si ₂ , 2(C ₂ H ₆ O) | C ₁₅ H ₁₄ | C ₂₁ H ₃₀ Si ₂ | |
| Temperature | 200(2) K | 180(2) K | 200(2) K | 200(2) K | |
| Crystal shape & Color | Prism, colorless | Prism, colorless | Prism, colorless | Prism, colorless | |
| Crystal size | 0.150 x 0.140 x 0.100 mm ³ | 0.200 x 0.100 x 0.080 mm ³ | 0.400 x 0.200 x 0.100 mm ³ | 0.300 x 0.150 x 0.100 mm ³ | |
| Formula weight / g mol ⁻¹ | 1005.82 | 1266.27 | 194.26 | 338.63 | |
| Crystal system | Triclinic | Monoclinic | Tetragonal | Monoclinic | |
| Space group | <i>P</i> -1 | <i>C</i> 2/ <i>c</i> | <i>I</i> 4 ₁ / <i>a</i> | <i>P</i> 2 ₁ / <i>c</i> | |
| Z | 2 | 8 | 16 | 4 | |
| Calculated density | 0.995 Mg/m ³ | 0.994 Mg/m ³ | 1.130 Mg/m ³ | 1.068 Mg/m ³ | |
| Cell parameter | <i>a</i> | 11.6403(14) Å | 34.1454(8) Å | 21.6843(2) Å | 14.1329(3) Å |
| | <i>b</i> | 18.4301(10) Å | 24.9090(6) Å | 21.6843(2) Å | 6.59460(10) Å |
| | <i>c</i> | 18.5637(16) Å | 22.8091(5) Å | 9.7108(2) Å | 23.4684(5) Å |
| | α | 60.565(11)° | 90° | 90° | 90° |
| | β | 80.343(15)° | 119.3180(10)° | 90° | 105.6690(10)° |
| | γ | 75.890(15)° | 90° | 90° | 90° |
| | <i>V</i> | 3358.3(8) Å ³ | 16915.0(7) Å ³ | 4566.10(13) Å ³ | 2105.99(7) Å ³ |
| F(000) | 1124 | 1140 | 1664 | 736 | |
| Absorption coefficient | 0.089 mm ⁻¹ | 0.676 mm ⁻¹ | 0.476 mm ⁻¹ | 1.491 mm ⁻¹ | |
| θ range for collection | 3.020 to 25.000° (MoK α) | 2.313 to 67.998° (CuK α) | 6.450 to 77.434° (CuK α) | 3.912 to 77.432° (CuK α) | |
| Index ranges | -13 ≤ <i>h</i> ≤ 13, -21 ≤ <i>k</i> ≤ 21, -22 ≤ <i>l</i> ≤ 22 | -40 ≤ <i>h</i> ≤ 41, -29 ≤ <i>k</i> ≤ 29, -27 ≤ <i>l</i> ≤ 27 | -27 ≤ <i>h</i> ≤ 24, -26 ≤ <i>k</i> ≤ 26, -12 ≤ <i>l</i> ≤ 11 | -16 ≤ <i>h</i> ≤ 17, -7 ≤ <i>k</i> ≤ 6, -29 ≤ <i>l</i> ≤ 28 | |
| Reflections collected | 51256 | 70491 | 18692 | 17125 | |
| Independent reflections | 11729 [R(int) = 0.1803] | 15353 [R(int) = 0.1011] | 2400 [R(int) = 0.0372] | 4309 [R(int) = 0.0296] | |
| Completeness | 99.3 % | 99.6 % | 99.6 % | 98.7 % | |
| Goodness-of-fit on F ² | 1.060 | 1.434 | 1.078 | 1.082 | |
| Final R indices [I > 2σ(I)] | R1 = 0.1248, wR2 = 0.3516 | R1 = 0.1390, wR2 = 0.3924 | R1 = 0.0536, wR2 = 0.1285 | R1 = 0.0410, wR2 = 0.1049 | |
| R indices (all data) | R1 = 0.2064, wR2 = 0.3847 | R1 = 0.1921, wR2 = 0.4429 | R1 = 0.0564, wR2 = 0.1311 | R1 = 0.0420, wR2 = 0.1059 | |

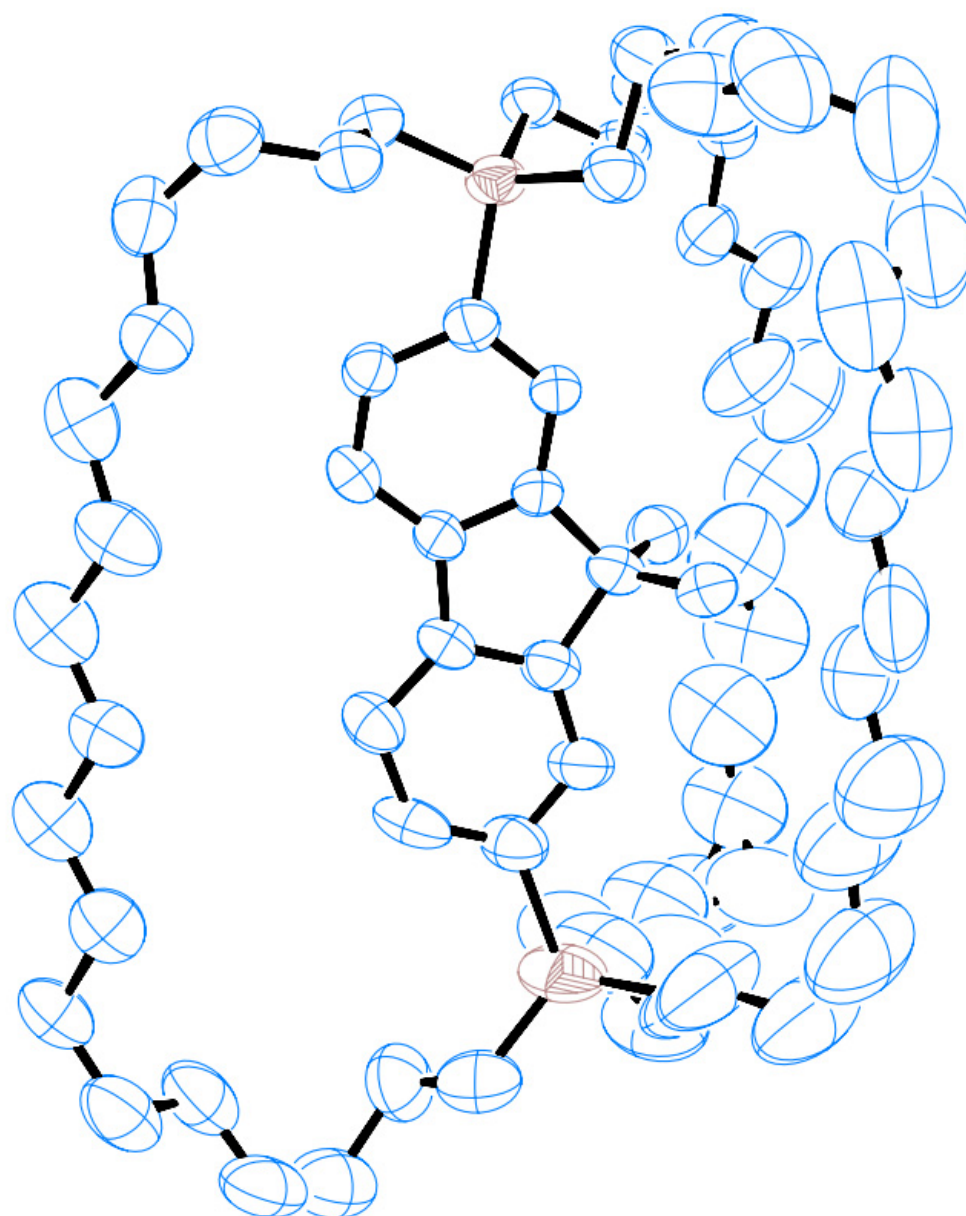


Fig. S37. An ORTEP drawing (30% thermal ellipsoids) of molecular structure of **C18** determined by X-ray crystallography.

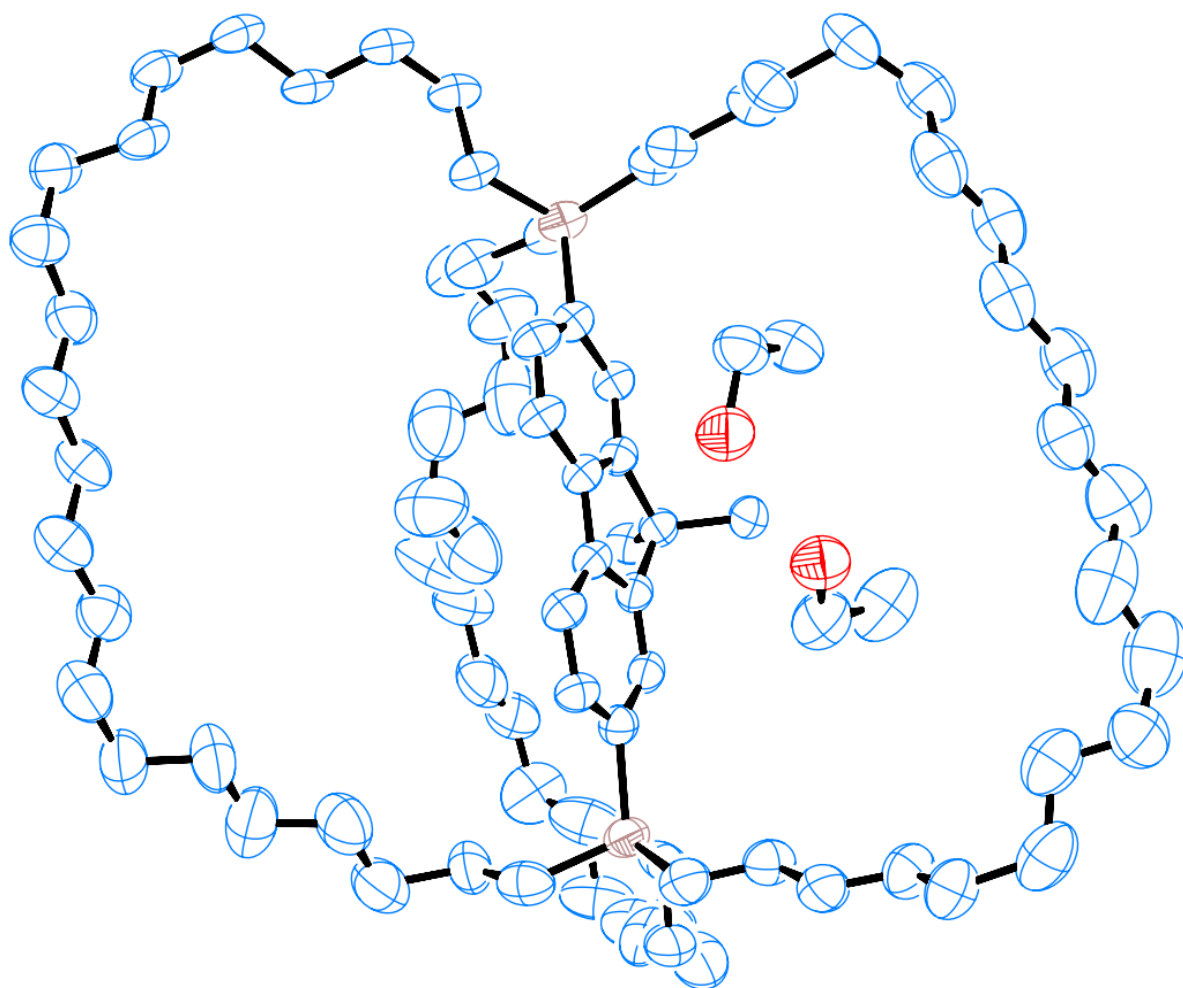


Fig. S38. An ORTEP drawing (30% thermal ellipsoids) of molecular structure of **C₂₂•2EtOH** determined by X-ray crystallography.

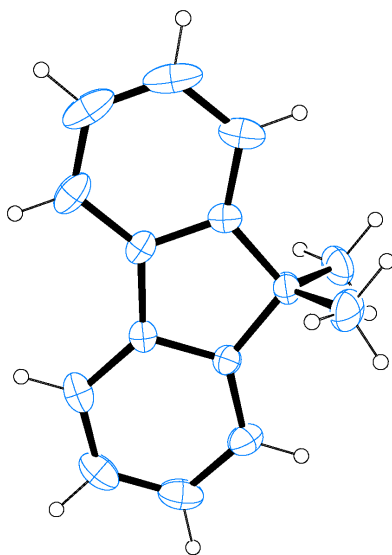


Fig. S39. An ORTEP drawing (30% thermal ellipsoids) of molecular structure of **Flu** determined by X-ray crystallography.

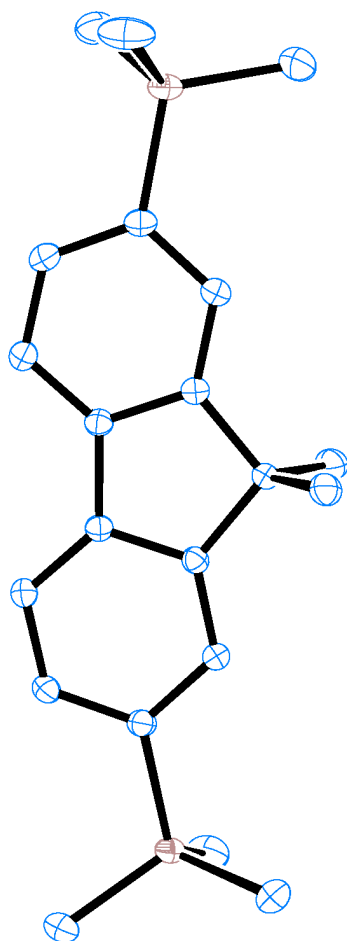


Fig. S40. An ORTEP drawing (30% thermal ellipsoids) of molecular structure of **TMS** determined by X-ray crystallography.

3. Appended Data of Fluorescence Measurements

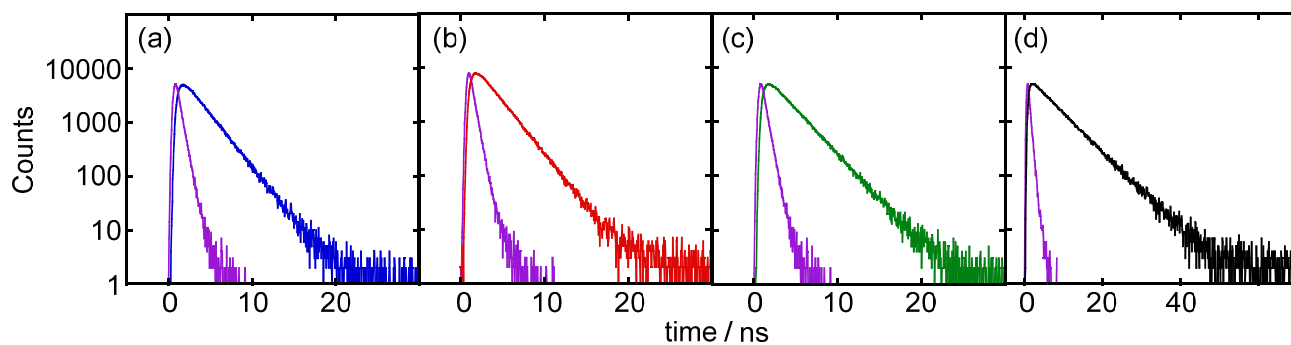


Fig. S41. Fluorescence life-time measurements for fluorenes in hexane (The excitation pulse was indicated with purple line.): (a) **C18**, (b) **C22**, (c) **TMS**, and (d) **Flu**.

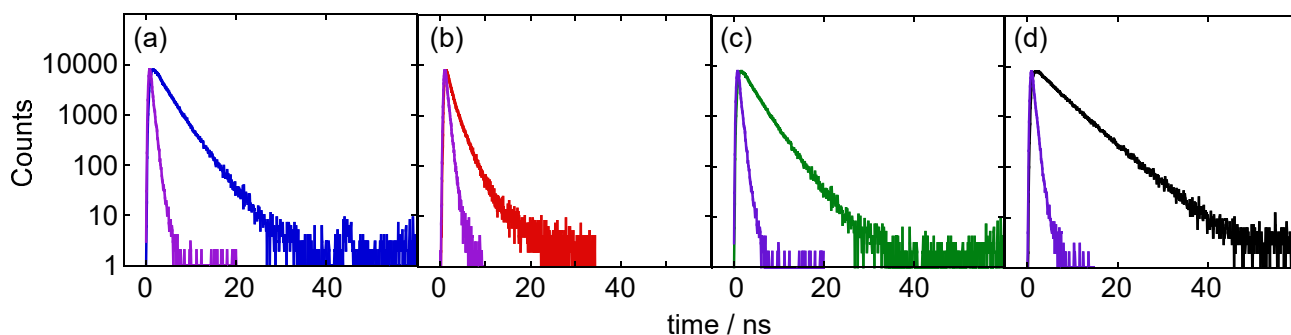


Fig. S42. Fluorescence life-time measurements for fluorenes in solid-states (The excitation pulse was indicated with purple line.): (a) **C18**, (b) **C22**, (c) **TMS**, and (d) **Flu**.

4. Appended Data of Solid-state ^2H NMR Study

a. Analysis of ^2H NMR spin-lattice relaxation (T_1) measurements

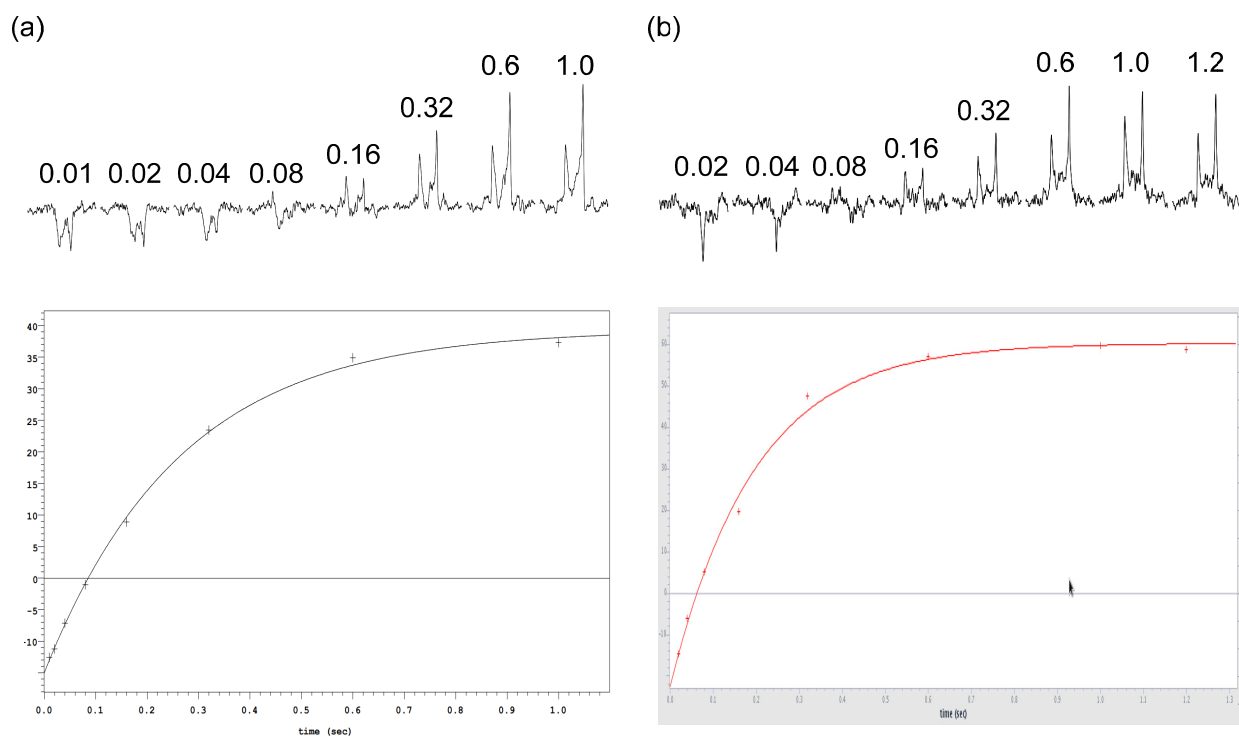


Figure S43 Inversion-recovery ^2H NMR spectroscopy data (300 K) and single exponential fit of (a) $\text{C18-}d_3$ and (b) $\text{C22-}d_3$.